Molecular Mechanisms Involved in Interleukin-1β Release by Macrophages Exposed to Metal Ions from Implantable Biomaterials

by

Maxime-Alexandre Ferko

Thesis submitted in partial fulfillment of the requirements for the degree of

MASTER OF APPLIED SCIENCE

in

Biomedical Engineering

Ottawa-Carleton Institute for Biomedical Engineering

University of Ottawa

Ottawa, Ontario, Canada

March 2018

Acknowledgements

Firstly, I would like to express my sincerest appreciation and gratitude to my thesis supervisor, Dr. Isabelle Catelas, for her expertise and tireless support and guidance throughout the completion of this thesis project. I am also extremely grateful for the opportunity she has given me to mentor and work closely with undergraduate thesis and co-op students. This was an invaluable experience and contributed greatly to my professional development.

I would like to thank my committee members, Dr. Xudong Cao, Dr. Rosalind Labow, and Dr. Katey Rayner for dedicating their time and effort into reviewing my thesis. Many thanks go to the members of the Orthopaedic Bioengineering Laboratory (OBL; Dr. Catelas' lab), especially Dr. Eric A. Lehoux, Research Associate in the lab. I cannot thank Dr. Lehoux enough for his willingness to share his technical expertise, his words of encouragement, and his kindness. My sincere thanks go to my fellow lab mates, Stephen Baskey, Zeina Salloum, and Ava Parsian, for their support and positivity. Special thanks go to Dr. Julie Joseph and Norah Alturki of Dr. Subash Sad's lab at the University of Ottawa for their help in getting my mouse model established.

I would also like to express my heartfelt gratitude to past undergraduate thesis and co-op students of the OBL who worked with me throughout my research project (Emily Ertel, Kriti Kumar, Jennifer Ham, and Hallie Arnott). Their help in the lab accelerated my project and made for a fun and positive atmosphere during long experiments.

Mes remerciements s'adressent également à tous les membres de ma famille pour leur soutien tout au long de mon cursus. Sans ce soutien, je n'aurais pas pu compléter ce projet. En particulier, je tiens à remercier ma mère (Dany), mon père (Jim), mon frère (Pierre-Olivier), ma grand-mère (Huguette), mon oncle (Pierre), et ma tante (Courtney). Je serai éternellement reconnaissant de leur appui.

Once again, I offer my deepest thanks to all that made this thesis possible.

Thesis Organization

This thesis is divided into six main chapters and includes one manuscript.

Chapter 1 introduces the context of the work.

Chapter 2 is the literature review focusing on biomaterials and orthopaedics, especially hip and knee implants; implant biomaterials properties and failure mechanisms; and finally, the inflammasome and the immune response to metal ions.

Chapter 3 describes the hypotheses and objectives of this thesis.

Chapter 4 is the manuscript. It focuses on the effects of metal ions from implantable biomaterials on the release of the pro-inflammatory cytokine IL-1β by macrophages, and analyzes if IL-1β release is dependent on caspase-1, oxidative stress and the NF-κB signaling pathway. More specifically, murine bone marrow-derived macrophages were exposed to cobalt(II), chromium(III), and nickel(II) ions, and the response (in terms of caspase-1 activation and IL-1β release) in the presence or absence of an inhibitor of caspase-1, oxidative stress, or NF-κB was studied.

Chapter 5 is the overall thesis discussion, which includes the conclusions from the work, technical considerations, and future studies.

Chapter 6 lists the references.

Abstract

Metal ions released from implantable biomaterials have been associated with adverse biological reactions that can limit implant longevity. Previous studies have shown that, in macrophages, Co^{2+}, Cr^{3+}, and Ni^{2+} can activate the NLR family pyrin domain-containing protein 3 (NLPR3) inflammasome, which is responsible for interleukin(IL)-1β production through caspase-1. Furthermore, these ions are known to induce oxidative stress, and inflammasome priming is known to involve nuclear factor kappa-light-chain-enhancer of activated B cells (NF-κB) signaling. However, the mechanisms of inflammasome activation by metal ions remain largely unknown. The objectives of this thesis were to determine if, in macrophages: 1. IL-1β release induced by metal ions is caspase-1-dependent; 2. caspase-1 activation and IL-1β release induced by metal ions are oxidative stress-dependent; and 3. IL-1β release induced by metal ions is NF-κB signaling pathway-dependent. Lipopolysaccharide (LPS)-primed murine bone-marrow-derived macrophages were exposed to Co^{2+}, Cr^{3+}, or Ni^{2+}, with or without an inhibitor of caspase-1, oxidative stress, or NF-κB. Culture supernatants were analyzed for active caspase-1 (immunoblotting) and/or IL-1β (ELISA). Overall, results showed that while both Cr^{3+} and Ni^{2+} may be inducing inflammasome activation, Cr^{3+} is likely a more potent activator, acting through oxidative stress and the NF-κB signaling pathway. Further elucidation of the activation mechanisms may facilitate the development of therapeutic approaches to modulate the inflammatory response to metal ions, and thereby increase implant longevity.

Table of Contents

Acknowledgements ..... **ii**
Thesis Organization ..... **iii**
Abstract ..... **iv**
List of Figures ..... **vii**
List of Tables ..... **viii**
List of Abbreviations ..... **ix**
1 Introduction **1**
2 Literature Review **3**
2.1 Biomaterials and Orthopaedics 3
2.1.1 Synovial Joints and Total Joint Arthroplasty 3
2.1.2 The Canadian Joint Replacement Registry (CJRR) 4
2.1.3 Hip Arthroplasty Implant Design 5
2.1.4 Knee Arthroplasty Implant Design 6
2.1.5 Cement and Implant Fixation 6
2.2 Implant Biomaterial Properties and Failure Mechanisms 6
2.2.1 Biomaterial Wear-induced Osteolysis and Aseptic Loosening 7
2.2.2 Evolution of Biomaterials in Total Joint Arthroplasty 7
2.2.3 Common Failure Mechanisms of Joint Replacements 9
2.3 The Inflammasome and the Immune Response to Metal Ions 12
2.3.1 Introduction to the NLRP3 Inflammasome 12
2.3.3 NLRP3 Inflammasome Priming 14
2.3.4 Mechanisms of NLRP3 Inflammasome Activation 16
3 Thesis Objectives and Hypotheses **21**
3.1 Objectives 21
3.2 Hypotheses 21
4 Manuscript **22**
4.1 Foreword 22
4.2 Abstract 22
4.3 Introduction 23

4.4 Materials and Methods 25
4.4.1 Metal Ions 25
4.4.2 Cells 25
4.4.3 Caspase-1 Enzyme Inhibition 26
4.4.4 Oxidative Stress Inhibition 27
4.4.5 NF-κB (p65) Transcription Factor Blocking 28
4.4.6 Cell Mortality Assessment 28
4.4.7 Statistical Analysis 29
4.5 Results 29
4.5.1 Effects of Caspase-1 Inhibitor (Z-WEHD-FMK) on IL-1β Release 29
4.5.2 Effects of Oxidative Stress Inhibitor (L-ascorbic acid) on Caspase-1 Activation and IL-1β Release 31
4.5.3 Effects of NF-κB Inhibitor (JSH-23) on IL-1β Release 32
4.6 Discussion 34
4.7 Acknowledgements 39
4.8 Supplementary Information 40
5 Thesis Discussion 43
5.1 Conclusions from the Work 43
5.2 Technical Considerations 44
5.2.1 Optimization of Bone Marrow-Derived Macrophage Generation 44
5.2.2 Analysis of Macrophage Phenotype by Flow Cytometry 46
5.2.3 Optimization of the Western Blotting Protocol for the Detection of Active Caspase-1 48
5.3 Future Studies 50
5.3.1 Inclusion of Additional Metal Ions and Metal Particles 50
5.3.2 Measurement of Intracellular Reactive Oxygen Species 51
5.3.3 Examination of Inflammasome Component Proteins 51
5.3.4 In Vivo Model of Osteolysis 52
6 References 54

List of Figures

Figure 1. Interleukin-1β (IL-1β) release by bone marrow-derived macrophages (BMDM) after exposure to (A) Cr^{3+}, (B) Ni^{2+}, or (C) Co^{2+}, with or without Z-WEHD-FMK **30**

Figure 2. Caspase-1 activation in bone marrow-derived macrophages (BMDM) after exposure to Cr^{3+}, Ni^{2+}, or Co^{2+}, with or without L-ascorbic acid (L-AA) **31**

Figure 3. Interleukin-1β (IL-1β) release by bone marrow-derived macrophages (BMDM) after exposure to (A) Cr^{3+}, (B) Ni^{2+}, or (C) Co^{2+}, with or without L-ascorbic acid (L-AA). **32**

Figure 4. Interleukin-1β (IL-1β) release by bone marrow-derived macrophages (BMDM) after exposure to Cr^{3+}, with or without JSH-23. ..... **33**

Supplementary Figure 1. Mortality of bone marrow-derived macrophages (BMDM) after exposure to Cr^{3+}, Ni^{2+}, or Co^{2+}, with or without Z-WEHD-FMK: (A, C and E) Percentages of dead cells; (B, D and F) Total numbers of cells (viable and dead). **40**

Supplementary Figure 2. Mortality of bone marrow-derived macrophages (BMDM) after exposure to Cr^{3+}, Ni^{2+}, or Co^{2+}, with or without L-AA: (A, C and E) Percentages of dead cells; (B, D and F) Total numbers of cells (viable and dead). **41**

Supplementary Figure 3. Mortality of bone marrow-derived macrophages (BMDM) after exposure to Cr^{3+} with or without JSH-23: (A) Percentages of dead cells; (B) Total numbers of cells (viable and dead) **42**

List of Tables

Table 1: Optimization of parameters for BMDM generation **46**
Table 2: Markers for flow cytometry **47**

List of Abbreviations

Abbreviation	Term
2-ME	Beta-mercaptoethanol
AAOS	American Academy of Orthopaedic Surgeons
AIM2	Absent in melanoma 2 protein
ALVAL	Aseptic, lymphocyte-dominated vasculitis-associated lesion
ANOVA	Analysis of variance
APAF-1	Apoptotic protease-activating factor-1
ASC	Apoptosis-associated speck-like protein
ATP	Adenosine triphosphate
BAPTA-AM	Bis-N,N,N',N'-tetraacetic acid-AM (calcium channel chelator)
BSA	Bovine serum albumin
CAPS	Cryopyrin-associated periodic syndromes
CARD	Caspase recruitment domain
CC	Ceramic-on-ceramic
CCAC	Canadian Council on Animal Care
CD	Cluster of differentiation
CGM	Complete growth medium
CJRR	Canadian Joint Replacement Registry
COA	Canadian Orthopaedic Association
CoCrMo	Cobalt-chrome-molybdenum (alloy)
DAMP	Danger-associated molecular pattern
DPBS	Dulbecco's phosphate-buffered saline
ECL	Enhanced chemiluminescence
ELISA	Enzyme-linked immunosorbent assay
ER	Endoplasmic reticulum
FBS	Fetal bovine serum
FC	Flow cytometer
HMDB	Hospital Morbidity Database

HR	Hip resurfacing
HRP	Horseradish peroxidase
HXLPE	Highly-crosslinked polyethylene
ICE	Interleukin-converting enzyme
IgG	Immunoglobin G
IKK	IκB kinase
IκBα	Inhibitor of NF-κB alpha
IL	Interleukin
IL-1R1	Interleukin-1 receptor type 1
IL-6	Interleukin-6
JSH-23	4-methyl-N1-(3-phenyl-propyl)-benzene-1,2-diamine
L-AA	L-ascorbic acid
LPS	Lipopolysaccharide
LRR	Leucine-rich repeat
M-CSF	Macrophage colony-stimulating factor
MoM	Metal-on-metal
MoPE	Metal-on-polyethylene
mtDNA	Mitochondrial DNA
NACRS	National Ambulatory Care Reporting System
NADPH	Nicotinamide adenine dinucleotide phosphate
NF-κB	Nuclear factor kappa-light-chain-enhancer of activated B cells
NIH	National Institutes of Health
NLR	NOD-like receptor
NLRC4	NLR family CARD domain-containing protein 4
NLRP1	NLR family pyrin domain-containing protein 1
NLRP3	NLR family pyrin domain-containing protein 3
NOD	Nucleotide oligomerization domain
P2X7R	P2X purinoreceptor 7
PAGE	Polyacrylamide gel electrophoresis
PAMP	Pathogen-associated molecular pattern
PBS	Phosphate-buffered saline

PMA	Phorbol 12-myristate 13-acetate
PMMA	Polymethyl methacrylate
PRR	Pattern recognition receptor
PVDF	Polyvinylidene fluoride
PYD	Pyrin domain
ROS	Reactive oxygen species
RPMI-1640	Roswell Park Memorial Institute formulation #1640 (media)
SDS	Sodium dodecyl sulfate
SPF	Specific pathogen-free
THR	Total hip replacement
Ti6Al4V	Titanium-6Aluminum-4Vanadium (alloy)
TJA	Total joint arthroplasty
TKA	Total knee arthroplasty
TLR	Toll-like receptor
TNF	Tumor necrosis factor
TNFR1	Tumor necrosis factor receptor 1
TNFR2	Tumor necrosis factor receptor 2
UHMWPE	Ultra-high molecular weight polyethylene
ULE	Ultra-low endotoxin
Z-WEHD-FMK	Z-Trp-Glu(OMe)-His-Asp(OMe)-fluoromethylketone

1 Introduction

Metal alloys have a long history of success in the field of implantable biomaterials (1). They can be found in many types of surgical implants, from the large components used to replace entire hip joints to the small fixtures used to anchor prosthetic teeth. Metals possess many properties befitting of a good biomaterial for many surgical applications, including excellent strength, fracture resistance, and cost (2,3). Moreover, metal alloys can be fabricated into complex shapes with relative ease while maintaining exacting manufacturing standards. However, over time, metal alloys release particles and ions through wear and corrosion processes (4,5). These wear and corrosion products can elicit host tissue reactions that can ultimately lead to implant failure and the need for corrective surgery (6–8).

In orthopaedics, the most common long-term cause of joint replacement failure is aseptic loosening of the implant following the loss of the surrounding bone support (9,10). The loosening is termed aseptic because no pathogenic organisms are involved. Decades of research into the problem has linked implant wear products (not exclusively metals) to the loss of bone surrounding the implant, termed periprosthetic osteolysis. In periodontology, a similar phenomenon of tooth implant loosening known as peri-implantitis is observed (11). In addition, metal wear and corrosion products, especially ions in the case of corrosion, may also be involved in other adverse tissue reactions seen in joint replacements, including hypersensitivity and pseudotumours (12–17). Clearly, metal wear products are linked to several problems of clinical interest. Therefore, their interaction with immune cells warrants further investigation.

Past *in vitro* studies, drawing from advances in research on the innate immune system, have linked metal implant wear and corrosion products to the oligomerization of an intracellular danger sensing platform known as the NLR family pyrin domain-containing protein 3 (NLRP3) inflammasome in macrophages (18,19). This inflammasome leads to the activation of a pro-interleukin(IL)-1β-cleaving enzyme known as caspase-1, whose product, mature IL-1β, has broad inflammatory effects which include periprosthetic osteolysis (20–22). The NLRP3 inflammasome is widely studied due to its ability to ‘sense’ many unrelated stimuli ranging from crystalline matter to pathogen-associated proteins, and its oligomerization relies on a two-step process dependent on the nuclear factor kappa-light-chain-enhancer of activated B cells (NF-κB) signaling pathway (23). The current body of research in immunology points to only a handful of

activation mechanisms, including reactive oxygen species (ROS) generation, K^+ efflux, and lysosomal rupture (23). In the biomaterials field, cell culture studies have shown that metal ions can lead to ROS production (24,25).

The potential relationship between metal ion-induced IL-1β and oxidative stress offers a promising research avenue to undercover new mechanisms involved in the biological response to implant wear and corrosion products that may lead to increased implant longevity. Indeed, a better understanding of how the innate immune system reacts to metal wear and corrosion products may influence the development of future implantable biomaterials as well as lay the foundation for pharmaceutic approaches designed to prevent, slow, or reverse adverse immune reactions.

2 Literature Review

2.1 Biomaterials and Orthopaedics

A biomaterial, as defined by the American National Institutes of Health (NIH), is “any substance or combination of substances, other than drugs, synthetic or natural in origin, which can be used for any period of time, and which augments or replaces partially or totally any tissue, organ, function of the body, in order to maintain or improve the quality of life of the individual” (26). They can improve quality of life by restoring a natural function, shortening recovery times, or serving as diagnostic and monitoring aids, among many other potential uses.

Ranked among the most successful and cost-effective of surgical innovations, total joint arthroplasties (TJA) are a class of orthopaedic surgeries that replace an arthritic or otherwise damaged joint in the body and restore its function while alleviating pain (27). A large part of the clinical success of joint arthroplasties is owed to the biomaterials used in the fabrication of the implants used to replace the natural joints, and a better understanding of how biomaterials interact with human tissues will pave the way for improved patient outcomes.

2.1.1 Synovial Joints and Total Joint Arthroplasty

The two most common types of arthroplasties are hip and knee replacements, according to the American Academy of Orthopaedic Surgeons (AAOS) (28). In Canada, hip and knee replacements are the second most common type of inpatient surgery after caesarian sections, with a combined total of over 116,000 patients operated on annually as of 2016 (29). While hip and knee replacements are most commonly indicated for degenerative conditions such as osteoarthritis and rheumatoid arthritis, they also may become necessary in cases of fracture, impingement, and even osteonecrosis in some cases (30).

Hip and knee joints are synovial joints, which are characterized by the presence of a fibrous capsule which envelops the joint (31,32). The synovial cavity, or volume surrounding the articulating ends of bones, is filled with synovial fluid, whose primary purpose is to reduce friction. The extremely low coefficient of friction found in synovial joints is also due to the presence of a layer of cartilage composed of collagen and proteoglycans (33). An important proteoglycan in the context of joints is lubricin, which coats the surface of articulating cartilage and provides boundary lubrication as the name implies (34).

The hip joint is a ball-and-socket joint. The ball is the femoral head and the socket is the pelvic acetabulum (32). The knee joint is a modified hinge joint with two articulations: one between the tibia and femur, the other between the femur and patella (knee cap) (31). Knee and hip joints are the largest and second largest joints in the body, respectively (35). Together, these joints are keys to locomotion. The implants used in hip and knee replacements replicate the functionality of the natural joints, a remarkable feat given that they are among the most mechanically loaded joints in the human body and experience very little friction.

In general, hip and knee replacements are successful procedures as evidenced by their prevalence and history of successful clinical results (36). However, the longevity of the implants is still of concern (10,37). The most common cause of long-term joint replacement failure is aseptic loosening secondary to periprosthetic osteolysis (38). Under this failure mode, an implant becomes loose in the absence of infection (aseptic) due to loss of surrounding bone (periprosthetic osteolysis). Affected patients must undergo revision surgery, a procedure more complex and costly than the primary joint replacement surgery due to the loss of bone stock (30).

2.1.2 The Canadian Joint Replacement Registry (CJRR)

The Canadian Joint Replacement Registry (CJRR), established in 2001 by the Canadian Institute for Health Information (CIHI) and the Canadian Orthopaedic Association (COA), aims to collect and analyze clinical information of primary and revision hip and knee replacements in Canada. It should be noted that the CJRR cannot track all hip and knee replacement surgeries in Canada, as only three provinces were mandated to report to the CJRR in 2014-2015 (Ontario, Manitoba, and British Columbia). Submissions from outside of these provinces are voluntary. The CJRR estimates its national procedure coverage to be 71.1% nationally for the 2014-2015 period, based on comparisons with the Hospital Morbidity Database (HMDB) and the National Ambulatory Care Reporting System (NACRS) (39). The trend appears to be for expanded coverage since the CJRR's coverage has improved significantly since the 2011-2012 period (when it was estimated to be just 42%), and Nova Scotia started mandating submission to the CJRR as of 2016. The most recent CJRR report, available for a 12-month period in 2014-2015, records 51,272 hip replacements and 61,421 knee replacement surgeries (39). This represents a 20.0% and 20.3% increase, respectively, compared to the previous 5 years. Of these surgeries, 4,347 were hip revisions and 4,185 were knee revisions, representing 8.5% and 6.8% of their respective totals.

The most common indication for both primary hip and knee replacements was degenerative arthritis (74.1% and 97.9%, respectively). The second most common indication for hip replacement was acute hip fracture (14.9%). Overall, degenerative arthritis, also known as osteoarthritis, is responsible for the large majority of joint replacements in Canada. Aseptic loosening of the implant was the most common indication for revision surgery, representing 28.0% of all hip revisions and 28.7% of all knee revisions. Other common indications included instability (16.5% for hip, 15.9% for knee) and infection (15.0% for hip, 23.4% for knee).

While total joint arthroplasty ranks among the most successful of surgical interventions, much can still be done to improve implant longevity and improve patient outcomes. Revision surgeries are more complex than primary surgeries, resulting in longer patient recovery times, lower likelihood of success in terms of pain alleviation and joint function restoration, and higher costs to the healthcare system (30). The most common indication for revision, aseptic loosening, is largely a result of implant wear product-mediated inflammation (9,10,40). Improvements in implant materials and designs in the past decades have led to a reduction in wear product generation. However, aseptic loosening remains a serious concern as evidenced by the above statistics. Efforts to understand the immune system response to wear products constitutes an active area of research, with long-term results potentially informing implant design and/or yielding pharmaceutical solutions to inflammation generated by these wear products.

2.1.3 Hip Arthroplasty Implant Design

Hip arthroplasty involves two types of implant devices: stem-type devices and hip resurfacing (HR). Stem-type devices will be referred to as total hip replacements (THR) in this thesis, to differentiate them from the HR. In a total replacement, the entirety of the femoral head and neck are removed, and a metal stem is inserted into the femur (35). The stem supports a new artificial femoral head fitted onto the neck of the stem. Older femoral component designs were non-modular (termed ‘monobloc’), and made leg length adjustments difficult at the time of implantation (41). The acetabular socket is roughened and fitted with a metallic cup containing a liner material designed to accept the femoral head component and allow rotation. HR differs from a THR only in the femoral component. Rather than excising the natural femoral head to allow for insertion of a stem and ball, the femoral head is reshaped to allow for the fitting of a

metallic surface cap (42). The suitability of a THR versus a HR depends on multiple patient factors including gender, age, weight, level of activity, and health of the bone stock.

2.1.4 Knee Arthroplasty Implant Design

Knee arthroplasty can be classified into three types: total knee replacement, unicompartmental (partial) knee replacement, and kneecap replacement (43). In a total knee replacement, the joint surfaces of the tibia and femur are cut and reshaped to allow for the fitting of the implant components (43). A tibial component covers the reshaped tibial end, while a curved femoral component covers the femoral end. A spacer component is placed between to permit smooth hinge articulation. Lastly, the under-surface of the kneecap, if affected by disease, is cut, reshaped and fitted with a surface component to allow smooth and pain-free motion over the replaced joint. Patients with bone damage (most commonly from osteoarthritis) limited to only one side of the knee or the under-surface of the patella (kneecap) may first be treated with partial or kneecap replacement, respectively (43).

2.1.5 Cement and Implant Fixation

Some designs of implants call for the use of fixation aids such as pins, screws, and bone cement (44,45). Advances in material engineering have led to the development of implant surface treatments that favor osseointegration, making cementless implants possible. In THR, the popularity of cementless design is such that only 17% of current hip replacements in Canada utilize bone cement for implant fixation (39). Conversely, cement fixation remains more common in total knee arthroplasty (TKA) in Canada (39). Notably, not all cementless designs perform identically. Indeed, a study of 20 different types of uncemented acetabular components including data from 7989 patients over a 20-year period at the Mayo Clinic concluded that significant differences exist in the long-term survival of these components (46).

2.2 Implant Biomaterial Properties and Failure Mechanisms

Biomaterials destined for use in joint arthroplasties are engineered for high strength, fracture toughness, fatigue resistance, corrosion and oxidation resistance, biocompatibility, and other factors (47,48). Currently, materials used for the implant fabrication include metal alloys, polyethylene, and ceramics. An important limitation with man-made biomaterials within the context of arthroplasty is the generation of wear products through normal use of the loaded articulating surfaces (49). Wear products can elicit an immune response ultimately resulting in

adverse events including periprosthetic osteolysis (which can lead to aseptic loosening) or hypersensitivity responses (mostly seen with metal wear products) (50). As such, the desire to reduce wear rates has been a driving force behind orthopaedic biomaterial evolution.

2.2.1 Biomaterial Wear-induced Osteolysis and Aseptic Loosening

Periprosthetic osteolysis, mainly a result of the inflammatory response to implant wear products, such as ultra-high molecular weight polyethylene (UHMWPE) particles or metal ions and particles, is regarded as a major failure mechanism (9,40,50,51). Although multifactorial in nature, with mechanical factors possibly involved (52), the literature consensus is that biomaterial-induced osteolysis and subsequent loosening is characterized by the slow but consistent release of wear products causing chronic inflammation in the surrounding tissues. In the early stages, symptoms may be absent or go unnoticed, but the worsening of osteolytic lesions over time can lead to implant migration (loosening) and failure (50). A key characteristic of biomaterial-induced osteolysis is its aseptic nature. Septic loosening, on the other hand, occurs as a result of bacterial infiltration (infection) at the implantation site (53). An implant ability to generate wear products in an artificial joint depends on the biomaterial used in its fabrication. These are reviewed in the following section.

2.2.2 Evolution of Biomaterials in Total Joint Arthroplasty

2.2.2.1 Ultra-High Molecular Weight Polyethylene (UHMWPE)

The first modern arthroplasty design introduced by Sir John Charnley in the 1960s used a metal alloy ball rotating in a polyethylene acetabular cup (54,55). The cup was sterilized by gamma radiation in air, and much of the early clinical success of this design was attributed to the polyethylene material (56). By the 1990s, manufacturers employed different sterilization processes to avoid polyethylene oxidation-related fatigue failures: gamma radiation in low oxygen air, and radiation-free processes such as gas plasma and chemical sterilization (56). Concern regarding oxidation and wear rates led to the development of highly-crosslinked polyethylene (HXLPE; clinically introduced in 1998) (56,57). HXLPE is more resistant to wear, but the crosslinking process can harm mechanical properties such as fracture and fatigue resistance (56,58). Currently, conventional UHMWPE is the most common bearing material found in joint replacements (59), and it is now being replaced by HXLPE. In Canada, UHMWPE and HXLPE accounted for approximately 17.7% and 55.2%, respectively, of all THR procedures

performed between 2003 and 2011 (60). HXLPE is so far performing well compared to UHMWPE based on reduced revision rates (61).

2.2.2.2 Ceramics

Ceramics are chemical compounds made of a metallic element such as aluminum or zirconium and a non-metallic element such as oxygen (62). Two common examples that have been used in joint bearings are aluminum oxide (alumina; Al_2O_3) and zirconium dioxide (zirconia; ZrO_2) (63). For example, the first ceramic-on-ceramic (CC) bearing described by Pierre Boutin in 1972 in France was made of alumina (64). Ceramics have useful material properties as bearing surfaces: they are extremely smooth, hard, bioinert and resistant to scratches, and possess good wettability which improves joint lubrication (62,63). This remarkable hardness comes, however, with increased fracture risks compared to metal alloys or polyethylene. However, newer ceramic composites have mitigated this risk. Modern ceramics in clinical use are in fact composites. For example, BIOLOX®delta material from Ceramtec is a composite made of 82% alumina, 17% zirconia, and small amounts of yttria and strontia (62). This composite is marketed as having improved fracture toughness compared to other ceramic materials. Furthermore, the bioinert property of ceramics combined with their very low wear rates has translated into extremely low incidence rates of wear-related osteolysis in patients with CC bearings (65,66). Nevertheless, CC bearings are less forgiving when it comes to component alignment by surgeons (67), which can result in squeaking and component fracture (67,68).

2.2.2.3 Metal Alloys

Like polyethylene, metal alloys are a founding material in joint arthroplasty. Today, the metal head in metal-on-polyethylene (MoPE) bearings is usually made of a metal alloy such as cobalt-chrome-molybdenum (CoCrMo) (69). Additionally, metal-on-metal (MoM) bearings are made of CoCrMo alloys (70). These MoM bearings possess very low volumetric wear rates, although the individual metal alloy wear particle size is very small. Indeed, studies report average diameters in the range of 30 to 100 nanometers (71–73). This is especially true when compared to conventional UHMWPE particles, which have been shown to have average diameters in the range of 0.4 to 1.2 micrometers (74–76). Despite the initial promise of MoM bearings to reduce revision rates due to lower volumetric wear rates and the possibility for larger diameter femoral heads for enhanced joint stability (77), recent clinical experience with the second generation of

MoM bearings has revealed significant biocompatibility problems leading to high early failure rates and subsequently action by regulatory bodies, lawsuits, and product recalls (54,78–80). The small size of metal alloy particles may be a contributing factor, especially given reports that MoM bearings release more individual particles despite their low volumetric wear rates compared to conventional UHMPE (81). Currently, MoM bearings in THR are regarded as no longer clinically viable (82). On the other hand, a role for MoM HR still exists for certain patients due to the unique advantages of HR procedures (such as the preservation of bone stock) (82).

Besides wear-related particle generation, which is possible for all bearing materials, metal alloys are uniquely susceptible to corrosion resulting in metal ion release. Metal ions can be released via the bearing articulation and as well as corrosion at the modular junctions of modern femoral stem designs (83,84). Indeed, the orthopaedic literature has coined the term "trunnionosis" to describe wear and corrosion of the modular femoral head-neck junction (83), and the long term systemic risks of metal ions such as Co^{2+} and Cr^{3+} released from implant alloys are not completely understood. Cobalt ion-related cardiomyopathy is an example of a related (though rare) serious health problem (85). Unfortunately, the problem of corrosion is not confined to MoM bearings, and the intersection of corrosion, tribology, and immunology still remains poorly outlined.

2.2.3 Common Failure Mechanisms of Joint Replacements

2.2.3.1 The Particle Disease Theory and the Innate Immune System

The link between wear particles and aseptic loosening was first proposed by Willert and Semlitsch in the 1970s (86). In the 1980s, polymethyl-methacrylate (PMMA) bone cement particles were thought to be chiefly involved, and the term cement disease was coined by the end of the decade (87). Finally, in 1994, Harris generalized the model to include all particles released from implant surfaces and coined the term particle disease (88). Briefly, the model of particle disease identifies the chronic inflammation associated with wear particle release as the cause of peri-prosthetic osteolysis and subsequent implant loosening. The inflammation causes increased osteoclastogenesis and impairs osteoblast production and function, and the net result is osteolysis near implant surfaces (50). Since 1994, studies seek to better understand the complex immunological pathways that result in osteolysis.

Macrophages are widely recognized as the principal cell type involved in the activation and maintenance of the inflammatory response (89–91). As phagocytic cells of the innate immune system (92), macrophages initiate a non-specific foreign-body response against wear particles and attempt to dispose of foreign material. However, particles made of common implant materials such as polyethylene, ceramic and metal alloys are not digestible, and macrophages can even form multinucleated foreign body giant cells in an attempt to sequester very large particles (93). As a result of the foreign body response, macrophages and other cells including dendritic cells release pro-inflammatory cytokines such as IL-1alpha (IL-1α) and IL-1β, tumor necrosis alpha (TNF)-alpha (TNF-α), and many others (40,94–97). These cytokines, which have been found in the periprosthetic tissues and synovial fluid of aseptically loosened joints (98,99), can stimulate mature osteoclast formation from macrophage-derived osteoclast precursors (10,100,101). Local imbalances at the level of osteoclasts and osteoblasts can then favor bone resorption (51). Studies have also shown that inflammation can impair the differentiation and function of osteoblasts (102–104), further tilting the imbalance in favor of bone resorption in the periprosthetic environment.

2.2.3.2 Wear Particle-induced Macrophage Activation

The mechanisms underlying wear particle-induced macrophage activation and pro-inflammatory cytokine release remain incompletely characterized, and constitute an area of active research. Macrophage pattern recognition receptors (PRR) seem likely to provide insight into this activation process. The toll-like receptor (TLR) and NOD-like receptor (NLR) families of PRR, which are surface and cytosolic receptor families, respectively, are of particular interest due to their ability to recognize a wide range of evolutionary-conserved molecular patterns from pathogens (pathogen-associated molecular pattern; PAMP), as well as endogenous danger ‘signals’ from necrotic or malfunctioning cells (danger-associated molecular patterns; DAMP) (105,106).

Importantly, TLR can mediate the activation of NF-κB (107), a rapid-acting transcription factor responsible for the upregulation of several pro-inflammatory cytokines including IL-1α, IL-1β, IL-6, TNF-α, and many others (108). TLR have been shown to be activated by wear products such as alkane polymers found in UHMWPE (109) as well as cobalt ions (110). It is also thought that PAMP (perhaps originating from subclinical implant biofilms (111)) can bind to wear

particles, potentially enabling their recognition by macrophage TLR (50). Similarly, NLRP3 has been shown to be activated by metal wear products such as particles and ions (18,19,112,113). Activation of NLRP3 leads to the assembly of the inflammasome, a key component of the innate immune system (114). Metal-ion induced NLRP3 inflammasome constitutes the focus of the present research project. Overall, a better understanding of innate immune system activation by wear products via TLR and NLR signaling is key to filling the knowledge gaps in particle disease theory.

2.2.3.3 Role of the Adaptive Immune System in Implant Failure

Adverse tissue responses mediated by the adaptive immune system in response to metal wear products are histopathologically different from the slow osteolysis process described above (50). These adverse responses are nonetheless aseptic and can include hypersensitivity reactions (17) and the development of tissue masses known as pseudotumours (12,14). Implication of the adaptive system in response to metal wear products is evidenced by histological studies reporting, in some cases, T and B lymphocytes as well as plasma cells (in addition to macrophages) in tissues surrounding MoM implants (99,115). Individual patient susceptibility to the adverse responses listed above appears to be highly variable and difficult to predict. Unknown hereditary factors may explain at least part of the variability (50).

Metal ions can elicit an adaptive response due to their capacity to act as haptens when forming organometallic complexes with proteins (50,116). The complete description of the adaptive response to metal haptens is highly complex and falls outside the scope of this review. It should be noted that metal wear products can also interact with the innate immune system (117), and that UHMWPE particles are not thought to activate the adaptive system (118).

2.2.3.4 Early Failure of Metal-on-Metal Hip Implant Designs

MoM bearings used in hip arthroplasty have generated increased concerns in the last few years due to reports of alarmingly high early failure rates compared to other bearing couples (78,119,120). Concerns over early failure led to safety communications from multiple regulatory bodies, including a May 2012 communication from Health Canada to orthopaedic surgeons and MoM patients (Identification number RA-190001071) (121). MoM designs have gradually fallen out of favor in Canada since their peak in the late 2000s (60), and the global interest in MoM has declined considerably as well (82).

The resurgence of MoM bearings throughout the 1990s was fueled in part by the desire for lower volumetric wear rates, which was predicted to result in fewer cases of aseptic loosening compared to more traditional polyethylene designs (54,122). As the high early failure rates and other complications (such as pseudotumour formation (12,115)) became more evident throughout the 2000s, researchers began to investigate the immunological underpinnings. In 2009, Caicedo et al. (18) reported that the inflammasome, a large complex involved in innate immune system activation, could be activated by metal particles and ions released by CoCrMo alloys. The inflammasome had been discovered by Martinon et al. (123) in 2002 and the remainder of the 2000s saw a rapid expansion in inflammasome literature.

Though the link between the inflammasome and metal ions was established within the context of hip implants, the finding is applicable to all implants made of metal alloys, including in the field of periodontology (11), as well as the field of allergology which attempts to understand how certain allergic reactions to metals are potentiated (124). Nevertheless, the molecular pathways that underlie metal ion-induced inflammasome activation and innate immune system activation are still poorly understood, and increased knowledge in this area is needed.

2.3 The Inflammasome and the Immune Response to Metal Ions

As key players in the innate immune system mission to maintain tissue homeostasis, inflammasomes are garnering increasing interest from several disciplines, including orthopaedic biomaterials. Inflammasomes can generate a potent pro-inflammatory response, such as the release of IL-1 family cytokines, after being assembled as a consequence of one of its constituent proteins sensing a signal(s) from PAMP and/or DAMP (125). In general, inflammasome complexes enable the activation of enzymes (such as caspase-1), which in turn process inactive pro-forms of pro-inflammatory cytokines into their mature active forms. These cytokines are of orthopaedic concern as they may lead to eventual periprosthetic osteolysis and subsequently implant failure by aseptic loosening.

2.3.1 Introduction to the NLRP3 Inflammasome

The history of the inflammasome can be traced back to the discovery of the caspase-1 enzyme in 1989 (126,127). It was initially named IL-1β-converting enzyme (ICE), owing to its ability to cleave pro-IL-1β into a smaller active form (128,129). In 1992, characterization studies revealed that active caspase-1 is composed of two subunits: the p10 and p20 subunits (130). How the

caspase-1 enzyme becomes active remained unknown until 2002, when Martinon et al. (123) described the first inflammasome. This 'early' inflammasome included caspase-1 and the NLR family pyrin domain-containing protein 1 (NLRP1), a member of the NOD-like receptor (NLR) family of intracellular pattern recognition receptors (PRR), and it was speculated that other NLR family members may form inflammasome complexes in response to a diverse array of stimuli. Indeed, in 2004, the NLRP3 inflammasome was first described in the context of research surrounding auto-inflammatory cryopyrin-associated periodic syndromes (CAPS) (131–133), further cementing the importance of the inflammasome as part of the innate immune system.

Currently, 3 of the 22 NLR family members reported to be present in humans are known to form inflammasome complexes, as does one member of the PYHIN family (114). Thus, four inflammasomes are well-established in literature: the NLRP1, NLRP3, NLR family CARD domain-containing protein 4 (NLRC4), and absent in melanoma 2 (AIM2) inflammasomes. Each inflammasome seems to have evolved to be activated by certain types of stimuli. The NLRP1 inflammasome is thought to mainly be activated in bacterial pathogen proteases (134,135), while the NLRC4 inflammasome is activated by intracellular bacteria proteins such as flagellin (136,137). The AIM2 inflammasome has been shown to bind to DNA and confers a method of defense against DNA viruses and cytosolic bacteria (138). The NLRP3 inflammasome is unique because of its capacity to be activated by wide array of structurally dissimilar agonists (23,139), many of which do not originate from pathogens. These agonists include pathogen-associated proteins such as malarial hemozoin (140), uric acid crystals (141), pore-forming toxins, asbestos (142), metal particles and ions (18,19,112,143), silica (144), aluminum (144), etc. Direct binding of all these agonists to the NLRP3 protein via any of its domains, such as its sensory leucine-rich repeat (LRR), pyrin domain (PYD), or nucleotide-binding NACHT (NACHT stands for domain present in NAIP, CIITA, HET-E, and TP-1) domain is regarded as highly structurally implausible (23,114,139,145). Therefore, research efforts have focused on identifying a common downstream activation mechanism of the NLRP3 inflammasome. To date, a few non-mutually exclusive activation mechanisms have been described, but there is no unifying consensus. Additionally, it is generally accepted that the formation of fully functional NLRP3 inflammasome requires a priming signal ahead of the activation signal (107,146).

The active NLRP3 inflammasome recruits pro-caspase-1 moieties that undergo autolytic processing into active caspase-1 due to their close proximity (139). Following activation, there is evidence to suggest that caspase-1 is secreted into the extracellular space along with mature IL-1β (147). Notably, it has also been suggested that NLRP3 and ASC may also be secreted (148). The purpose of caspase-1 and inflammasome component secretion is not fully understood, though it is possible that this process serves to convert pro-caspase-1 and pro-IL-1β released from nearby necrotic cells into their active forms (149).

The NLRP3 inflammasome has been described as the most intensively studied inflammasome (114), perhaps in part due to its activation complexity and the role it plays in various inflammatory diseases. More specifically, in the context of this thesis, the NLRP3 inflammasome has been shown to be the specific type of inflammasome involved in orthopaedic wear product inflammation (18).

2.3.3 NLRP3 Inflammasome Priming

2.3.3.1 Immunological Background

The necessity of priming for NLRP3 inflammasome activation was first reported in 2009 by Bauernfeind et al. (107). Priming ensures an upregulation of NLRP3 protein and pro-IL-1β through the activation of NF-κB, and is necessary because the basal level of NLRP3 and pro-IL-1β are insufficient for efficient inflammasome assembly and subsequent mature IL-1β production. Indeed, *de novo* protein synthesis has been described as a limiting step for NLRP3 inflammasome activation (107). The need for priming prior to inflammasome activation is postulated to function as a regulatory checkpoint, ensuring that the inflammasome may only be activated in cases where the release of potent cytokines like IL-1β is warranted (23,114). The existence of auto-inflammatory diseases related to improperly controlled NLRP3 inflammasome activation, such as CAPS, supports this notion.

Priming hinges on activation of NF-κB, and therefore priming stimuli includes ligands for receptors capable of activating NF-κB, including the TLR, NLR, tumor necrosis factor receptor 1 (TNFR1), TNFR2, and IL-1 receptor 1 (IL-1R1) (107,150). Lipopolysaccharide (LPS) is commonly used as a standard priming stimulus for *in vitro* inflammasome research (151,152). Its ability to activate NF-κB and therefore induce NLRP3 and pro-IL-1β expression has been reported to be wholly dependent on its receptor TLR4 (107). It is important to note that *in vivo*,

any number of ligands for the receptors mentioned above may be responsible for priming. Additionally, it has been reported that priming may be self-limiting through negative regulation of the NF-κB pathway (153). Interestingly, Gurung et al. (151) have found that prolonged LPS exposure (12 to 24 hours) is relatively ineffective as a priming step compared to acute exposure (up to 4 hours), and reported that chronic TLR stimulation leads to NLRP3 inflammasome down-regulation through IL-10 signaling.

Interestingly, it has been observed by Juliana et al. (154) that NLRP3 inflammasome activation could be achieved after just 10 minutes of priming with LPS, which is an insufficient amount of time for *de novo* synthesis of inflammasome components. The authors described a new post-translational priming mechanism, where pattern recognition receptor (PRR) signaling leads to the deubiquitination of the leucine-rich repeat (LRR) domain of cytosolic basal NLRP3, which is otherwise maintained in an inactive ubiquitinated state incapable of oligomerization. The authors also found that cells expressing high levels of NLRP3 did not require priming by LPS (and therefore did not require post-translational deubiquitination of NLRP3) in order to be later activated by ATP. To explain this, the authors suggested that at high expression levels, NLRP3 might be only partially ubiquitinated and therefore may be capable of oligomerization and inflammasome assembly. This finding supports the importance of transcriptional priming, as originally described by Bauernfeind et al. (107). In general, immunological studies on NLRP3 inflammasome priming support the existence of both transcriptional and post-translational priming mechanisms, and the necessity of priming is well-established. The complete picture of the involved molecular pathways is nonetheless highly complex and remains to be fully elucidated.

2.3.3.2 Significance of Priming in Orthopaedic Studies

Noteworthily, there has been some degree of discordance in orthopaedic literature regarding the role of priming for metal ion- and metal particle-induced NLRP3 inflammasome activation. Multiple studies by Caicedo et al. (18,19,112), including their original report of inflammasome involvement in the immune response to orthopaedic wear products (18), make no mention of priming and do not describe priming incubations in their methodology. Similarly, a later study by the same group reported no significant increase in osteolysis in a murine calvaria model when using CoCr particles with LPS compared to just using CoCr particles (113). However, these

studies contrast with the work of Bi et al. (155,156) and Greenfield et al. (157,158), who attributed a large portion of the immune reactivity of titanium particles to the presence of adherent endotoxin. For example, Bi et al. (155) showed that endotoxin removal from particle surfaces resulted in a 50 to 70% reduction in osteolysis while the re-addition of LPS restored the original osteolytic capacity of the particles. Subsequent studies by Greenfield et al. (157) and Manzano et al. (159) corroborated these results. Greenfield et al. (158) have also proposed that endogenous alarmins do not significantly contribute to the immune reactivity of metal particles, and that the involved TLR cognates are bacterially-derived PAMP. In the case of aseptic loosening, the lack of an apparent infection or bacterial source casts some uncertainty on this proposal. However, it has been suggested that sub-clinical bacterial biofilms may exist on implant surfaces (50,111). Though asymptomatic and difficult to detect, they may be a source of priming PAMP capable of potentiating strong immune responses against wear particles. Interestingly, a recent study by Samelko et al. (160) has reported that the presence of LPS alongside CoCrMo particles induced a two-fold increase in osteolysis compared to CoCrMo particles alone in a murine calvaria model. These results, which support the involvement of TLR, are somewhat contrary to the previous studies from the same group (18,19,112,113).

Overall, while there remains some ambiguity regarding the role of priming in metal ion- and metal particle-induced inflammasome activation within the orthopaedic literature, most studies suggest that priming is required.

2.3.4 Mechanisms of NLRP3 Inflammasome Activation

The activators of the NLRP3 inflammasome are numerous and structurally diverse, can be exogenous or endogenous, and can act upon a cell or cause damage in different ways (23,114). As stated previously, the great structural diversity of the activators makes the direct sensing (or binding) of all of these activators by NLRP3 extremely unlikely. Instead, it is possible that the multitude of disparate initial activator effects, which are upstream of NLRP3 activation, boil down to a smaller number (or possibly just one) unifying downstream mechanism(s) that eventually lead(s) to NLRP3 activation (139). The bulk of NLRP3 inflammasome research has thus focused on the identification of these common downstream mechanisms, with the aim of uncovering the final NLRP3 activation signal. Despite over a decade of research, the complete picture of the molecular pathways surrounding NLRP3 activation remains unclear. Perhaps the

three most widely accepted common downstream mechanisms engendered by inflammasome activators are cation fluxes (specifically K^+ efflux), lysosomal disruption, and mitochondrial dysfunction involving the generation of ROS.

2.3.4.1 Cation Flux

Potassium ion efflux has been identified as a necessary mechanism for NLRP3 activation by several activators including nigericin, a microbial toxin, and extracellular ATP (161–163). Both have been known to result in mature IL-1β in LPS-stimulated cells due to their capacity to decrease intracellular levels of K^+ since well before the discovery of the inflammasome (164), and today they are commonly used as NLRP3 activators for *in vitro* studies (151,152). Nigericin functions as a potassium ionophore (165). More specifically, it is an antiporter of K^+ and H^+. ATP, on the other hand, binds to receptor P2X7R on the surface of the cell membrane, which promotes the opening of pores allowing Na+ and Ca^+ influx along with K^+ efflux (166,167). Notably, only ATP depends on P2X7R for potassium efflux leading to inflammasome activation (114). Other activators cause K^+ efflux via entirely different mechanisms, highlighting the distinctiveness of mechanisms far upstream of NLRP3 activation.

Interestingly, calcium ions have also recently been linked to NLRP3 inflammasome activation, as Ca^{2+} has been shown to act as a discrete inflammasome activator at elevated extracellular concentrations (168–170). Also, it has been shown that some NLRP3 inflammasome activators rely on the release of Ca^{2+} into the cytosol from intracellular stores (171). Thus, it is possible that Ca^{2+} fluxes are involved in one or more common inflammasome activation pathways, in much the same way as K^+ fluxes. Another possibility is that K^+ and Ca^{2+} fluxes are two sides of the same coin. Indeed, both fluxes may be required and complement each other, or only one flux may act on NLRP3 activation while the other represents a reciprocal flux necessary to maintain overall balance (114). The latter possibility has previously been suggested by Murakami et al. (170), who showed that Ca^{2+} shift into the cytosol caused by inflammasome activator ATP was blocked by high extracellular K^+, and by Muñoz-Planillo et al. (163), who demonstrated that inflammasome activation by high extracellular Ca^{2+} was blocked by high extracellular K^+.

Interestingly, nickel ions (Ni^{2+}) have been shown to activate the inflammasome in a manner dependent on K^+ and Ca^{2+} fluxes (172). Li et al. (172) have demonstrated that NLRP3 inflammasome activation (indirectly measured via IL-1β release) was greatly diminished when

LPS-primed macrophages were treated with Ni^{2+} in the presence of high extracellular KCl. Similarly, inflammasome activation by Ni^{2+} was blocked when macrophages were pre-treated with intracellular calcium chelator Bis-N,N,N',N'-tetraacetic acid-AM (BAPTA-AM). Taken together, the authors surmised that both K^+ efflux and Ca^{2+} were required for Ni^{2+}-induced NLRP3 inflammasome activation. This finding is plausible given the current state of knowledge surrounding cation fluxes described above.

Overall, cation flux mechanisms surrounding NLRP3 inflammasome activation remain unclear, and there is a lack of consensus regarding the exact role of K^+ and Ca^{2+} (114,149). For example, some reports demonstrate that high extracellular K^+ could not prevent cytosolic Ca^{2+} influx, which is inconsistent with the reports described above (173,174). At least part of the difficulties in understanding how cation fluxes mediate inflammasome activation may be explained by the limitations in real time ion monitoring methods, as indicated by Yaron et al. (175).

2.3.4.2 Lysosomal Disruption and Orthopaedic Wear Particles

NLRP3 inflammasome activation may occur as a result of the phagocytosis of undigestible particulate matter such as carbon nanotubes (176), silica (144,150), asbestos (142), metal alloy particles (19,112,113), and aluminum salts (144). Frustrated phagocytosis of these kinds of undigestible matter can lead to lysosomal rupture and loss of contents (including various enzymes) (144). Lysosomal rupture induced in the absence of particulates has been shown to lead to inflammasome activation (144), suggesting that at least some particulates activate the inflammasome principally by lysosomal rupture secondary to frustrated phagocytosis. Cathepsins, low-pH proteases mainly found within lysosomes, appear to be involved in NLRP3 activation following lysosomal rupture (112,144,177–179). Specifically, a cathepsin B inhibitor has been found effective at inhibiting NLRP3 inflammasome activation by particulate matter (180). Notably, K^+ efflux has been found to be essential for NLRP3 activation by several particulates, although no mechanism has been suggested to link lysosomal rupture to downstream K^+ efflux (149).

Unsurprisingly, IL-1β production induced by micrometer-sized CoCrMo particles has been linked to lysosomal destabilization and the NLRP3 inflammasome (112). Furthermore, this IL-1β production was found to be dependent on the lysosomal protein cathepsin B, corroborating the results of Hornung et al. (144), who showed that NRLP3 activation by silica crystals and

aluminum salts occurred through the same mechanisms. In support of the lysosomal destabilization model, it was also reported that CoCrMo particles of larger size (micrometer range) and more irregular surfaces induced higher levels of IL-1β release (112). It is conceivable that all undigestible wear particles activate the NLRP3 inflammasome via the same lysosomal destabilization mechanisms regardless of the material type. However, it should be noted that metal particles may release ions which can aggravate the inflammatory response.

2.3.4.3 Reaction Oxygen Species, Mitochondrial Damage, and Metal Ions

The link between NLRP3 inflammasome activation and organelles was first suggested by Hornung et al. (181), who investigated inflammasome activation by lysosomal damage. This suggestion was later substantiated by another study (182). More specifically, the authors reported that an excess of ROS was necessary for NLRP3 inflammasome activation, and pointed to the mitochondria as highly important organelles for inflammasome activation, considering that mitochondria are a primary source of ROS. In addition, the authors also pointed to the role of mitochondrial dysfunction due to an abnormal transmembrane potential as an important factor in inflammasome activation. This study changed the landscape of NLRP3 inflammasome research, as subsequent studies sought to expound on these findings. For example, a study of Nakahira et al. (183) suggested that mitochondrial DNA (mtDNA) (whose presence in the cytosol can indicate a dysfunction) is required to activate the NLRP3 inflammasome. The authors demonstrated that priming with LPS followed by activation with ATP led to cytosolic mtDNA release, an interesting finding given that oxidized mtDNA was later shown to be capable of binding to NLRP3 and causing inflammasome assembly (184). In addition, the authors reported that cells deficient in NLRP3 did not display the expected signs of mitochondrial dysfunction (mtDNA release and abnormal mitochondrial transmembrane potential) following priming and activation treatments, suggesting that NLRP3 may be more than simply acting as a sensor downstream of mitochondrial dysfunction. Additional links between mitochondria and NLRP3 activation have recently been revealed by study from Misawa et al. (185), who reported that NLRP3 must be co-located with the mitochondria (where ASC is localized at rest) in order for inflammasome assembly to begin. Interestingly, the authors also showed that inactive NLRP3 resides within the endoplasmic reticulum (ER), thus a mechanism for NLRP3 vectoring is likely to exist. It remains unclear how ion flux and/or ROS are involved in NLRP3 displacement towards the mitochondria, although the authors suggested that mitochondrial damage can

indirectly lead to excessively high levels of acetylated alpha-tubulin, enabling microtubules to shift mitochondria closer to the nucleus and the ER.

Of note, it is possible that ROS and mitochondrial damage in the context of inflammasome activation may not be inextricably linked. For example, the inflammasome activator linezolid (an antibiotic) has been shown to cause inflammasome activation through mitochondrial dysfunction independently of mitochondrial ROS (186). Relatedly, there is evidence to support the notion that the degree of mitochondrial dysfunction, as defined by the transmembrane potential, is an important factor in inflammasome activation (187). Furthermore, a recent study by Sang et al. (188) reported that vitamin C, a ROS inhibitor, inhibits NRLP3 inflammasome activation by scavenging mitochondrial ROS. Overall, findings point to ROS and/or mitochondrial damage being sufficient for inflammasome activation, though often these occur concomitantly.

ROS may an important role in the case of metal ion-induced inflammasome activation. Caicedo et al. (18) reported that metal ion-induced IL-1β release was decreased in the presence of an inhibitor of nicotinamide adenine dinucleotide phosphate (NADPH) oxidase, whose primary catalytic function is intracellular ROS production (189). In immunological literature, NADPH oxidase initially appeared to be an important source of ROS linked with inflammasome activation (142). However, subsequent studies casted doubt on this model by demonstrating that cells deficient in this oxidase could still efficiently produce IL-1β (144,190). Metal ion-induced ROS, if indeed responsible for NRLP3 activation and not related to NADPH oxidase, may instead be a product of ion reactivity within the cytosol and/or a result of ion-induced mitochondrial damage. In line with this notion, studies have shown that Cr^{3+} are capable of superoxide, hydrogen peroxide, and hydroxyl radical production through redox cycling (191), and several studies have demonstrated the cytotoxic potential of Co^{2+} and Cr^{3+} (94,97,192–194). Nevertheless, further experimental work is required to confirm the involvement and nature of reactive oxygen species in metal ion-induced NLRP3 inflammasome activation.

3 Thesis Objectives and Hypotheses

3.1 Objectives

The overall objective of this research was to identify molecular mechanisms that lead to caspase-1 activation and IL-1β release in the presence of metal ions. Results could lead to the development of therapeutic approaches for the modulation of chronic inflammation leading to aseptic loosening of implants. The specific objectives of this thesis were to:

1. Determine if, in macrophages, IL-1β release induced by Co^{2+}, Cr^{3+}, or Ni^{2+} is caspase-1-dependent;
2. Determine if, in macrophages, caspase-1 activation and IL-1β release induced by Co^{2+}, Cr^{3+}, or Ni^{2+} are oxidative stress-dependent;
3. Determine if, in macrophages, IL-1β release induced by Co^{2+}, Cr^{3+}, or Ni^{2+} is NF-κB signaling pathway-dependent.

The first objective intended to verify the involvement of caspase-1 in metal ion-induced IL-1β release in our system (using murine bone marrow-derived macrophages), and served as a pre-requisite for the second objective. The second objective specifically analyzed metal ion-induced oxidative stress as a potential intracellular signal capable of eliciting caspase-1 activation that has been linked to inflammasome activation, and ultimately IL-1β release. The third objective analyzed the role of the NF-κB signaling pathway (which is known to be involved in the inflammasome pathway) in metal ion-induced IL-1β release. Together, these objectives provide insights into the molecular mechanisms involved in the release of the pro-inflammatory cytokine IL-1β by macrophages in response to metal ions.

3.2 Hypotheses

1. IL-1β release by macrophages after exposure to Co^{2+}, Cr^{3+} or Ni^{2+} is dependent on caspase-1;
2. Oxidative stress caused by Co^{2+}, Cr^{3+}, or Ni^{2+} in macrophages leads to caspase-1 activation and subsequently IL-1β release;
3. IL-1β release by macrophages after exposure to Co^{2+}, Cr^{3+}, or Ni^{2+} is dependent on the NF-κB signaling pathway.

4 Manuscript

4.1 Foreword

As described in the literature review, the potential relationship between metal ion-induced IL-1β and oxidative stress offers a promising research avenue to uncover new mechanisms involved in the biological response to implant wear and corrosion products. A better understanding of these mechanisms may lead to increased implant longevity. The focus of this thesis was to provide insight into the molecular mechanisms involved in the release of the pro-inflammatory cytokine IL-1β by macrophages in response to metal ions.

The results of this work are included in a manuscript entitled:

"Effects of metal ions on caspase-1 activation and IL-1β release in murine bone marrow-derived macrophages", by Maxime-Alexandre Ferko and Isabelle Catelas.

This manuscript was recently submitted for publication in the PLoS ONE journal. All data were obtained by myself, with the exception of three experiments with Ni^{2+} (data used to generate Figure 1B and Supplementary Figures 1C & 1D), which were obtained by Emily Ertel (undergraduate student in the lab). All data were analyzed by myself. The manuscript was written by myself and reviewed by my supervisor, Dr. Isabelle Catelas.

4.2 Abstract

Ions released from metal implants have been associated with adverse tissue reactions and are therefore a major concern. Studies with macrophages have shown that cobalt, chromium, and nickel ions can activate the NLRP3 inflammasome, a multiprotein complex responsible for the activation of caspase-1 (a pro-interleukin (IL)-1β-cleaving enzyme). However, the mechanism(s) of inflammasome activation by metal ions remain largely unknown. The objectives of this study were twofold: 1. to determine if, in macrophages, metal ion-induced caspase-1 activation and IL-1β release are oxidative stress-dependent; and 2. to determine if metal ion-induced IL-1β release is dependent on NF-κB. Lipopolysaccharide (LPS)-primed murine bone marrow-derived macrophages (BMDM) were exposed to Co^{2+} (6-48 ppm), Cr^{3+} (100-500 ppm), or Ni^{2+} (12-96 ppm) with or without an inhibitor of caspase-1 (Z-WEHD-FMK), oxidative stress (L-ascorbic acid; L-AA), or NF-κB (JSH-23). Cell culture supernatants were analyzed for active caspase-1 by western blot and/or IL-1β release by ELISA. Immunoblotting revealed the presence of the

cleaved active caspase-1 p20 subunit in supernatants of BMDM incubated with Cr^{3+}, but not with Ni^{2+} or Co^{2+}. When 2 mM L-AA was present with Cr^{3+}, the cleaved subunit was undetectable and IL-1β release decreased down to the level of the negative control, demonstrating that caspase-1 activation by Cr^{3+} was oxidative stress-dependent. ELISA showed that Cr^{3+} induced the highest release of IL-1β, while Co^{2+} had limited or non-significant effects. The addition of 2 mM L-AA induced a decrease in IL-1β release with both Cr^{3+} and Ni^{2+}, down to or below the level of the negative control. Finally, when present during both priming with LPS and activation with Cr^{3+}, JSH-23 blocked IL-1β release, demonstrating NF-κB involvement. Overall, this study showed that while both Cr^{3+} and Ni^{2+} may be inducing inflammasome activation, Cr^{3+} is likely a more potent activator, dependent on oxidative stress and with the involvement of NF-κB.

4.3 Introduction

Implantable metal alloys such as cobalt-chromium-molybdenum (CoCrMo) and stainless steel are widely used in medical devices, especially in hip and knee replacements (195). However, material degradation through corrosion and wear mechanisms may compromise the structural integrity of the implants, and the biologic effects of the wear and corrosion products are of great clinical concern (196,197). Ion release from the alloy components is particularly concerning, as elevated levels of metal ions have been reported in the serum, synovial fluid, and blood of patients with joint implants (198–200). In addition, corrosion at the modular interfaces of joint implants have been associated with early adverse tissue reactions (201,202), including hypersensitivity reactions (203) and pseudotumours (12,15,204), and the long-term release of wear products can lead to a chronic inflammation, and thereby periprosthetic osteolysis (40,91,205). Overall, a better understanding of the molecular mechanisms leading to the inflammatory response to wear and corrosion products is necessary to develop potential therapeutic treatments as well as to facilitate the development of more compatible and durable biomaterial alloys.

Previous *in vitro* studies have shown that metal ions including Co^{2+}, Cr^{3+}, and Ni^{2+} can trigger the assembly of the NLR family pyrin domain-containing protein 3 (NLRP3) inflammasome (18,19,172) in macrophages, the predominant cell type in periprosthetic tissues (91,206,207). The NLRP3 inflammasome has become the most widely studied member of the inflammasome

family since its discovery in 2002 (123) due to its capacity to be activated by a wide array of structurally dissimilar danger-associated molecular patterns (DAMP) and pathogen-associated molecular patterns (PAMP) (140,141,144). It is a large multiprotein complex responsible for the release of mature interleukin (IL)-1β, a cytokine that plays a key role in inflammation, and it is tightly regulated through a two-step process referred to as priming and activation (23,145). During the priming step, a PAMP binds to a toll-like receptor (TLR) type of pathogen recognition receptor (PRR) on the cell membrane surface (107), leading to the upregulation of pro-IL-1β and NLRP3 through the nuclear factor kappa-light-chain-enhancer of activated B cells (NF-κB) pathway (107). During the activation step, a PAMP or DAMP causes NLRP3 to oligomerize and recruit ASC (apoptosis-associated speck-like protein containing a CARD), which itself recruits pro-caspase-1 enzyme (23,114). The recruitment of pro-caspase-1 enzyme leads to its activation into cleaved caspase-1, which then cleaves pro-IL-1β into mature IL-1β.

While previous studies have shown that Co^{2+}, Cr^{3+}, and Ni^{2+} can trigger the assembly of NLRP3 inflammasome (18,19,172), the underlying mechanisms of activation remain largely unknown and constitute an active area of research in various research fields including orthopaedics, periodontology (11), and allergology (124,172). Basic immunological research has revealed that NLRP3 induction relies on NF-κB signaling (107), and that several DAMP can activate the NLRP3 inflammasome through reactive oxygen species (ROS) production, K^+ efflux, lysosomal rupture, and/or spatial rearrangement of organelles (23,114). Metal ions are known to adversely affect cellular function, as evidenced by their cytotoxicity (94,97,193). More specifically, Co^{2+}, Cr^{3+}, and Ni^{2+} have been shown to induce an increase in ROS production in immune cells *in vitro* (24,25), as well as IL-1β release in macrophages (18,19,172). Interestingly, IL-1β release induced by metal ions has been shown to decrease in the presence of an inhibitor of nicotinamide adenine dinucleotide phosphate (NADPH) oxidase (18), whose primary catalytic function is ROS production (189). It is therefore possible that these metal ions activate the NLRP3 inflammasome through ROS production, following NF- κB activation.

The objectives of the present study were twofold: 1. to determine if, in macrophages, metal ion-induced caspase-1 activation and IL-1β release are oxidative stress-dependent; and 2. to determine if metal ion-induced IL-1β release is dependent on the NF-κB pathway. Overall, this

study provides insights into the mechanisms of metal ion-induced NLRP3 inflammasome activation in macrophages.

4.4 Materials and Methods

4.4.1 Metal Ions

Stock solutions of Co^{2+}, Cr^{3+}, and Ni^{2+} were prepared fresh, as previously described (194). Briefly, $CoCl_2 \cdot 6H_2O$ (≥99.5% purity; Fisher Scientific, Waltham, MA), $CrCl_3 \cdot 6H_2O$ (≥99.2% purity; Sigma, St Louis, MO), and $NiCl_2 \cdot 6H_2O$ (≥99.999% purity; Sigma) were dissolved in cell culture-grade water (Lonza, Walkersville, MD), and the solutions were sterilized by filtration through 0.2-μm pore size cellulose acetate syringe filters (VWR, Mississauga, ON).

4.4.2 Cells

Bone marrow-derived macrophages (BMDM) were differentiated from bone marrow cells isolated from the femura, tibiae, and coxal bones of 4- to 16-week-old female wild type C57BL/6J mice (The Jackson Laboratory, Bar Harbor, ME). Procedures were approved by the University of Ottawa Animal Care Committee (Protocol ME-2350). The University of Ottawa animal care and use program meets the Canadian Council on Animal Care (CCAC) guidelines and is licensed under the Province of Ontario Animals for Research Act. The mice were cared for and housed at the Animal Care Facility of the University of Ottawa, a specific-pathogen-free (SPF) facility. More specifically, mice (up to four per cage) were housed in individually ventilated cages (Sealsafe®; Techniplast, West Chester, PA) with 6-mm size corncob bedding (Envigo RMS, Indianapolis, IN), cotton fiber-based nesting material (Ancare, Bellmore, NY), and a shreddable refuge hut (Ketchum, Brockville, ON). The animals were maintained at 22^0C and a relative humidity of 40% under a 12h-light:12h-dark photoperiod with *ad libitum* access to food (Teklad Global 18% Protein Rodent Diet; Envigo RMS) and water (purified by reverse osmosis and acidified to pH 2.5-3.0 with hydrochloric acid). Euthanasia was performed by CO_2 gas asphyxiation followed by cervical dislocation, and all efforts were made to minimize suffering. Euthanized mice were soaked in 70% (v/v) ethanol immediately prior to dissection.

After careful dissection and isolation of bones, bone marrow was flushed atop of a 100-μm nylon mesh cell strainer (Fisher Scientific) using a 27G x ½" needle-syringe (BD Biosciences, Durham, NC) filled with growth medium for bone marrow cell differentiation consisting of RPMI 1640 including L-glutamine (Wisent, St-Bruno, QC), supplemented with 8% heat-inactivated ultra-low

endotoxin fetal bovine serum (FBS) (NBSF-701; North Bio, Toronto, ON), 100 U/mL Penicillin-Streptomycin (Thermo Fisher, Waltham, MA), and 0.1% beta-mercaptoethanol (2-ME) (Thermo Fisher). Strained bone marrow cells were centrifuged at 150 ***g*** for 10 min at room temperature (RT), and resuspended in the above growth medium at 1.5 x 10^6 cells/mL. Suspension-type dishes of size 100/15-mm (Greiner Bio-One, Monroe, NC) were thinly coated by a 50-μL droplet of growth medium containing 50 ng recombinant macrophage-colony stimulating factor (M-CSF) (R&D Systems, Minneapolis, MN) using a disposable bacterial cell spreader (Excel Scientific, Victoriaville, CA), immediately prior to being seeded with 10 mL of cell suspension per dish. The dishes were then incubated for 6 days in a humidified environment at 37^0C and 5% CO_2.

At the end of the incubation, non-adherent cells were removed by rinsing the dishes with 5 mL of the above growth medium, and mature adherent BMDM were harvested by light pressure washing of the dish surfaces with a 10-mL Class A volumetric pipette (SIBATA Scientific Technology, Saitama, Japan). The collected BMDM were centrifuged at 300 ***g*** for 10 min at RT, then resuspended at 1 x 10^6 cells/mL in regular growth medium (growth medium defined above but without 2-ME). Twenty-four (24)-well tissue culture plates (Greiner Bio-One) were then seeded with 0.3 mL of cell suspension per well and incubated 4h under cell culture conditions to allow cell attachment. Unless otherwise stated, at the end of the incubation, the cell supernatants were discarded and the adherent BMDM in each well were primed by exposure to 500 ng/mL lipopolysaccharide (LPS) (Sigma) for 6h under cell culture conditions.

4.4.3 Caspase-1 Enzyme Inhibition

At the end of the incubation for priming, the medium containing LPS was replaced with regular growth medium containing 0 or 20 μM Z-WEHD-FMK (R&D Systems), an irreversible caspase-1 inhibitor, and the cells were incubated 1h under cell culture conditions. Co^{2+} (6 to 48 ppm final concentrations), Cr^{3+} (100 to 500 ppm), Ni^{2+} (12 to 96 ppm), nigericin (5 μM; positive control), or cell-culture grade water (ion solvent) (negative control) was then added to the cell supernatants and the cells were incubated an additional 18 to 24h. At the end of the incubation, supernatants were collected, centrifuged at 300 ***g*** for 10 min at 4^0C, snap-frozen in liquid nitrogen, and stored at -80^0C for later analysis of IL-1β release by enzyme-linked immunosorbent assay (ELISA).

Freshly thawed culture supernatants were gently mixed and concentrations of IL-1β were measured by ELISA using the Mouse IL-1 beta Uncoated ELISA Kit (Thermo Fisher), as per the manufacturer's instructions. Absorbance measurements were performed at 450 nm using a hybrid microplate reader (Synergy™ 4; BioTek, Winooski, VT). The reference wavelength at 570 nm was subtracted from the measurements. The nominal minimum concentration of IL-1β detectable by ELISA was 8 pg/mL, as per the manufacturer's specifications.

4.4.4 Oxidative Stress Inhibition

At the end of the incubation for priming, the medium containing LPS was replaced with regular growth medium containing 0 or 2 mM L-ascorbic acid (L-AA) (Sigma), an oxidative stress inhibitor, and the cells were incubated 1h under cell culture conditions. Co^{2+} (18 ppm final concentration), Cr^{3+} (300 ppm), Ni^{2+} (48 ppm), nigericin (5 μM; positive control), or cell-culture grade water (negative control) was then added to the cell supernatants and the cells were incubated an additional 18 to 24h. At the end of the incubation, supernatants were collected, centrifuged at 300 ***g*** for 10 min at 4^0C, snap-frozen in liquid nitrogen, and stored at -80^0C for later analysis of active caspase-1 and IL-1β release by western blot (as detailed below) and ELISA (as described above), respectively.

Freshly thawed culture supernatants were vortex-mixed, and protein determination was performed using the bicinchoninic acid colorimetric assay with bovine serum albumin (BSA) as the protein standard (Thermo Fisher). Absorbance (562 nm) was measured using a hybrid microplate reader (Synergy™ 4; BioTek). Aliquots (30 μg protein) of the culture supernatants were mixed with 4X Laemmli sample buffer, and analyzed by sodium dodecyl sulfate (SDS)-polyacrylamide gel electrophoresis (PAGE) using precast mini-format tris-glycine gradient (8-16%) gels (Bio-Rad, Hercules, CA). Pre-stained protein molecular weight standards (Bio-Rad) were used. For western blotting, proteins were electrotransferred onto a 0.45-μm pore size polyvinylidene fluoride (PVDF) membrane (Millipore, Billerica, MA). The blotted membrane was reversibly stained for total protein with 0.1% (w/v) Ponceau S (BP103-10; Fisher Scientific) in 5% (v/v) acetic acid (Fisher Scientific). Tris-buffered saline (TBS; 20 mM Tris base [Fisher Scientific], 130 mM NaCl [Fisher Scientific], pH 7.6) containing 5% immunoanalytical-grade non-fat dry milk (Blotto®; Rockland Inc., Limerick, PA), and TBS were used as the blocking and antibody dilution buffer, respectively. The primary antibody, a mouse anti-caspase-1 p20 subunit

monoclonal antibody (AG-20B-0042-C100; Adipogen Corporation, San Diego, CA), and secondary antibody, a polyclonal anti-mouse IgG horseradish peroxidase (HRP) conjugate (W4021; Promega Corporation, Madison, WI), were used at a dilution of 1:1000 and 1:5000, respectively. Chemiluminescence detection was performed using ECL (enhanced chemiluminescent) HRP substrate (Millipore), as per the manufacturer's instructions, and the blots were imaged using a near-infrared fluorescence/chemiluminescence imaging system (Odyssey Fc; LI-COR Biosciences, Lincoln, NE).

4.4.5 NF-κB (p65) Transcription Factor Blocking

At the end of the incubation for cell attachment, the culture supernatants were replaced with regular growth medium containing 0 or 60 μM JSH-23 (i.e., 4-methyl-N1-(3-phenylpropyl)-1,2-benzenediamine; Cayman Chemical, Ann Arbor, MI), an NF-κB transcription factor inhibitor, and the cells were incubated 1h under cell culture conditions. LPS (500 ng/mL final concentration) was then added to each well and the cells were incubated 6h under cell culture conditions. At the end of this incubation, the culture supernatants were replaced with regular growth medium containing 0 or 60 μM JSH-23, and the cells were incubated another 1h. Cr^{3+} (300 ppm final concentration), nigericin (5 μM; positive control), or cell culture-grade water (negative control) was then added to the cell supernatants and the cells were incubated an additional 18 to 24h. In total, four JSH-23 conditions were tested: no JSH-23, JSH-23 present exclusively during the priming incubation with LPS, JSH-23 present exclusively during the activation incubation with Cr^{3+} or nigericin, and JSH-23 present during both incubations. At the end of the 18 to 24h incubation, supernatants were collected, centrifuged at 300 ***g*** for 10 min at 4^0C, snap-frozen in liquid nitrogen, and stored at -80^0C for IL-1β measurements by ELISA, as described above.

4.4.6 Cell Mortality Assessment

At the end of the experiments, adherent cells were washed with 0.5 mL/well of ice-cold Dulbecco's Phosphate Buffered Saline (DPBS) (Sigma), incubated 15 min at RT in 300 μL of Accutase® (Thermo Fisher), and detached by gentle pipetting using a 1-mL manual single-channel pipette (Mettler Toledo, Columbus, OH). The cell suspensions were transferred into 2-mL untreated polystyrene culture tubes (Axygen Scientific, Union City, CA), and cell mortality was analyzed by dye-exclusion hemocytometry under phase contrast microscopy using trypan

blue (0.04% [w/v] final concentration; Sigma) and an improved Neubauer hemocytometer (Hausser Scientific, Horsham, PA).

4.4.7 Statistical Analysis

Statistical analysis was performed in SPSS v24.0 (IBM, Armonk, NY) using additive two-way analysis of variance (ANOVA), with ion concentration as a fixed effect and experiment as a random effect, and Tukey-Kramer post-hoc pairwise tests. $p<0.05$ was considered significant.

4.5 Results

4.5.1 Effects of Caspase-1 Inhibitor (Z-WEHD-FMK) on IL-1β Release

ELISA results revealed the highest increase in IL-1β release with Cr^{3+}, up to 1280% with 300 ppm ($p<0.001$), relative to the negative control (cells with no ions and no Z-WEHD-FMK) (Fig 1A). The increase was not significant with 500 ppm Cr^{3+}, likely due to the higher toxicity of Cr^{3+} at this elevated concentration. IL-1β release also increased with Ni^{2+}, up to 265% with 48 ppm ($p<0.001$), relative to the negative control (Fig 1B). As with Cr^{3+}, the release decreased with higher Ni^{2+} concentrations, likely reflecting a higher toxicity of Ni^{2+} as concentration increases. Finally, incubation with Co^{2+} revealed a small but statistically significant increase in IL-1β release, up to 64% with 18 ppm and 24 ppm ($p<0.001$), relative to the negative control (Fig 1C). The increase was not significant with 48 ppm, once again likely reflecting the higher toxicity of Co^{2+} at this elevated concentration. Interestingly, a decrease of 36% was observed with 6 ppm Co^{2+} ($p<0.001$).

The presence of 20 μM Z-WEHD-FMK induced a decrease of 76% to 86% in IL-1β release with 200 to 400 ppm Cr^{3+} ($p<0.001$ in all cases) (Fig 1A), down to levels similar to that of the negative control. It also induced a decrease of 35% to 45% with 48 ppm Ni^{2+} or higher ($p\leq0.002$ in all cases) (Fig 1B). Finally, it induced a decrease with 6 ppm Co^{2+}, down to levels below the detection threshold, and a decrease of 40% to 48% with 12 to 24 ppm Co^{2+} ($p<0.001$ in all cases), down to levels similar to that of the negative control (Fig 1C).

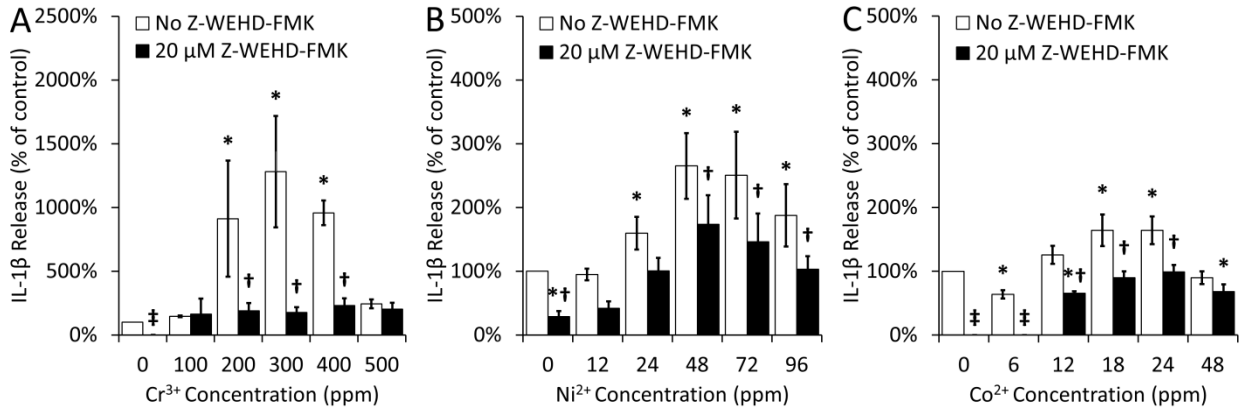

Figure 1. Interleukin-1β (IL-1β) release by bone marrow-derived macrophages (BMDM) after exposure to (A) Cr^{3+}, (B) Ni^{2+}, or (C) Co^{2+}, with or without Z-WEHD-FMK. Cells were incubated with the indicated concentrations of ions for 18 to 24h with or without 20 μM Z-WEHD-FMK (caspase-1 inhibitor) under cell culture conditions after a 6h priming incubation with 500 ng/mL of lipopolysaccharide (LPS). Cell culture supernatants were analyzed by ELISA. IL-1β release is expressed as a percentage of the release in the negative control (cells with no ions and no Z-WEHD-FMK). An asterisk (*) indicates a significant difference ($p<0.05$) between a given ion concentration with or without Z-WEHD-FMK and the negative control. A dagger (†) indicates a significant difference ($p<0.05$) between a given ion concentration with Z-WEHD-FMK and the same ion concentration without Z-WEHD-FMK. A double dagger (‡) indicates that the measurement was below the detection threshold. Data are presented as means ± SEM of 3-5 independent experiments performed in triplicate.

Trypan blue dye-exclusion analysis revealed an ion concentration-dependent increase in the percentages of dead cells, up to 52% with 500 ppm Cr^{3+} ($p<0.001$) (Supplementary Fig 1A; see section 4.8), 70% with 96 ppm Ni^{2+} ($p<0.001$) (Supplementary Fig 1C), and 71% with 48 ppm Co^{2+} ($p<0.001$) (Supplementary Fig 1E), relative to the negative control (cells with no ions and no Z-WEHD-FMK). The total number of cells (live and dead) decreased by up to 27% with 400 and 500 ppm Cr^{3+} (Supplementary Fig 1B), 50% with 96 ppm Ni^{2+} (Supplementary Fig 1D), and 27% with 48 ppm Co^{2+} (Supplementary Fig 1F) ($p<0.001$ in all cases). Of note is that the presence of 20 μM Z-WEHD-FMK did not have any significant effect on the percentage of dead cells with Cr^{3+} and Ni^{2+} (Supplementary Fig 1A and 1C) and decreased it with 24 ppm Co^{2+} (from 56% to 51%; $p=0.025$) and 48 ppm Co^{2+} (from 71% to 65%; $p=0.006$) (Supplementary Fig 1E). Finally, the presence of 20 μM Z-WEHD-FMK also did not induce any significant differences in the total number of cells, except with 200 ppm Cr^{3+} (Supplementary Fig 1B).

Overall, Z-WEHD-FMK was considered to have minimum toxic effects in the conditions analyzed.

4.5.2 Effects of Oxidative Stress Inhibitor (L-ascorbic acid) on Caspase-1 Activation and IL-1β Release

Immunoblotting results revealed the presence of the cleaved p20 subunit of caspase-1 in the supernatant of cells incubated with 300 ppm Cr^{3+}, but not with 48 ppm Ni^{2+} or 18 ppm Co^{2+} (Fig 2). Additionally, pro-caspase-1 was less abundant in BMDM cultured with Cr^{3+} compared to BMDM cultured with Ni^{2+} or Co^{2+}. Importantly, the cleaved p20 subunit, present with 300 ppm Cr^{3+}, was undetectable when 2 mM L-AA was also present.

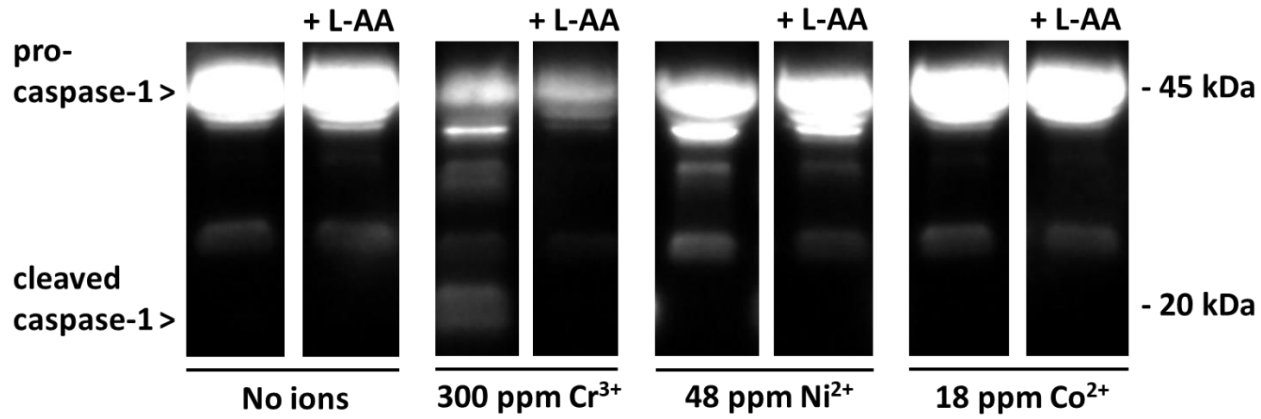

Figure 2. Caspase-1 activation in bone marrow-derived macrophages (BMDM) after exposure to Cr^{3+}, Ni^{2+}, or Co^{2+}, with or without L-ascorbic acid (L-AA). Cells were incubated with the indicated ion concentrations for 18 to 24h with or without 2 mM L-AA under cell culture conditions after a 6h priming incubation with 500 ng/mL of lipopolysaccharide (LPS). Cell culture supernatants were analyzed by western blotting for detection of the cleaved (active) caspase-1 subunit p20. Immunoblot is representative of three independent experiments.

ELISA results showed that the presence of 2 mM L-AA induced a decrease of 92% in IL-1β release with 300 ppm Cr^{3+} ($p<0.001$; Fig. 3A), as well as a decrease of 67% with 48 ppm Ni^{2+} ($p<0.001$; Fig 3B), down to or below the level of the negative control (cells with no ions and no L-AA), respectively. Co^{2+} (18 ppm) did not induce significant IL-1β increase (Fig 3C).

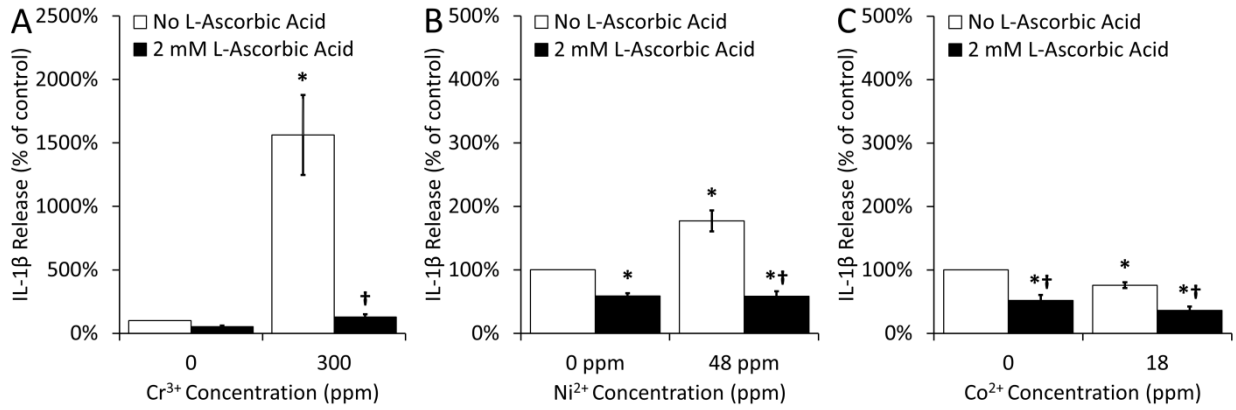

Figure 3. Interleukin-1β (IL-1β) release by bone marrow-derived macrophages (BMDM) after exposure to (A) Cr^{3+}, (B) Ni^{2+}, or (C) Co^{2+}, with or without L-ascorbic acid (L-AA). Cells were incubated with the indicated ion concentrations for 18 to 24h with or without 2 mM L-AA (oxidative stress inhibitor) under cell culture conditions after a 6h priming incubation with 500 ng/mL of lipopolysaccharide (LPS). Cell culture supernatants were analyzed by ELISA. IL-1β is expressed as percentage of the release in the negative control (cells with no ions and no L-AA). An asterisk (*) indicates a significant difference ($p<0.05$) between a given ion concentration with or without L-AA and the negative control. A dagger (†) indicates a significant difference ($p<0.05$) between a given concentration with L-AA and the same concentration without L-AA. Data are presented as means ± SEM of 3 independent experiments performed in triplicate.

Of note is that while the presence of 2 mM L-AA did not induce any significant differences in the percentage of dead cells with 300 ppm Cr^{3+} and 48 ppm Ni^{2+} (Supplementary Fig 2A and 2C, respectively; see section 4.8), it induced a small but significant increase in the percentage of dead cells with 18 ppm Co^{2+} (from 39% to 45%; $p=0.012$) (Supplementary Fig 2E). Finally, while the presence of 2 mM L-AA induced a small but significant decrease in the total number of cells with 300 ppm Cr^{3+} (from 65% to 52%, relative to the negative control; $p=0.026$) (Supplementary Fig 2B), the differences were not significant with 48 ppm Ni^{2+} and 18 ppm Co^{2+} (Supplementary Fig 2D and 2F, respectively). Overall, L-AA was considered to have minimum toxic effects in the conditions analyzed.

4.5.3 Effects of NF-κB Inhibitor (JSH-23) on IL-1β Release

ELISA results revealed that when present during both the 6h-LPS priming incubation and the 18 to 24h incubation with Cr^{3+}, 60 μM JSH-23 induced a decrease of 89% in IL-1β release ($p<0.001$), down to the level of the negative control (cells with no ions and no JSH-23) (Fig 4). When present during either the 6h-LPS priming incubation or the 18 to 24h incubation with Cr^{3+},

60 μM JSH-23 induced only a partial decrease of 67% and 65% in IL-1β release ($p<0.001$ in both cases), respectively, and the levels remained higher than those in the negative control. The presence of JSH-23 did not have a significant effect in the negative control.

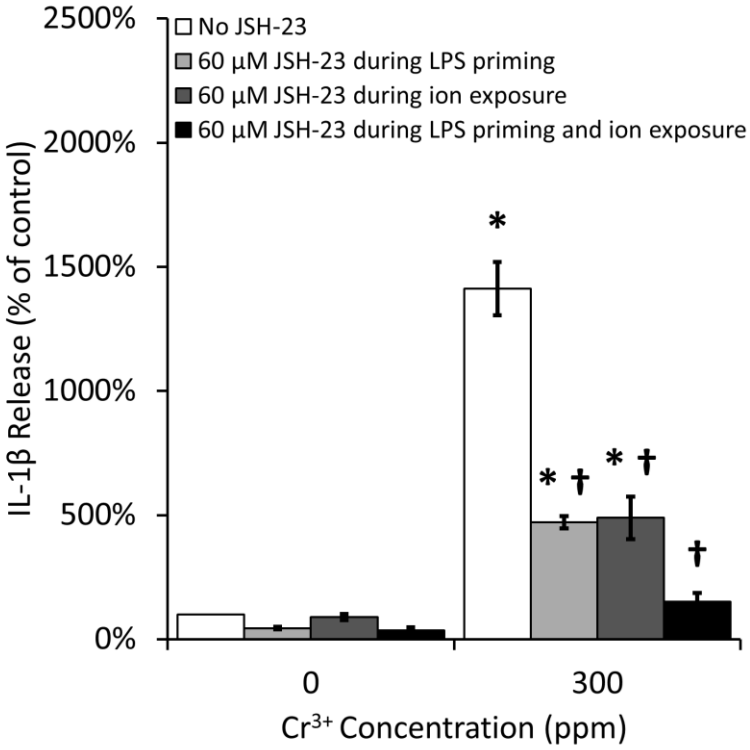

Figure 4. Interleukin-1β (IL-1β) release by bone marrow-derived macrophages (BMDM) after exposure to Cr^{3+}, with or without JSH-23. Cells were incubated with 300 ppm Cr^{3+} for 18 to 24h with or without 60 μM JSH-23 (NF-κB inhibitor) under cell culture conditions after a 6h priming incubation with 500 ng/mL of lipopolysaccharide (LPS). In total, four JSH-23 conditions were tested: no JSH-23 (white bars), JSH-23 present exclusively during the priming incubation with LPS (light gray bars), JSH-23 present exclusively during the incubation with Cr^{3+} ions (dark gray bars), and JSH-23 present during both incubations (black bars). Cell culture supernatants were analyzed by ELISA. IL-1β is expressed as a percentage of the release in the negative control (cells with no ions and no JSH-23). An asterisk (*) indicates a significant difference ($p<0.05$) between a given ion concentration with or without JSH-23 and the negative control. A dagger (†) indicates a significant difference ($p<0.05$) between a given ion concentration with JSH-23 and the same concentration without JSH-23. Data are presented as means ± SEM of 3 independent experiments performed in triplicate.

Of note is that when present during both the LPS priming incubation and the ion incubation, 60 μM JSH-23 induced a small but significant increase in the percentage of dead cells in the negative control (from 6% to 12%; $p<0.001$) (Supplementary Fig 3A; see section 4.8), along

with a significant decrease in the total number of cells (from 100% to 84%; $p<0.001$) (Supplementary Fig 3B). However, it did not induce any significant differences in the percentage of dead cells and in the total number of cells with 300 ppm Cr^{3+} (Supplementary Fig 3A and 3B, respectively). Overall JSH-23 was considered to have minimum toxic effects in the conditions analyzed.

4.6 Discussion

The present study analyzed the effects of Co^{2+}, Cr^{3+} and Ni^{2+} on caspase-1 activation and IL-1β release (probable indicator of inflammasome assembly) in BMDM. This study focused on the effects of Co^{2+}, Cr^{3+} and Ni^{2+} because these ions are released from wear and corrosion of CoCrMo and stainless steel alloys (widely used in orthopaedic applications) and remain a major cause for concern (12,15,201–204). The ranges of ion concentrations were based on: 1. past *in vitro* studies analyzing metal ion-induced macrophage cytotoxicity and cytokine release (94,97,192,193); 2. the assumption that macrophage stimulation is likely to require higher concentrations of stimulating agent *in vitro* than it does *in vivo* (where cells are exposed to multiple stimulating factors simultaneously); and 3. the assumption that the concentration of these ions is higher in periprosthetic tissues than in body fluids where their concentrations are in the ppb range (193).

Macrophages have been shown to be the predominant cell type in periprosthetic tissues (91,206,207). As part of the innate immune system front line, they interact with wear particles and metal ions and secrete pro-inflammatory cytokines (208). While the subsequent chain of events leading to periprosthetic osteolysis is well described in the literature (10,40,51), the molecular mechanisms of macrophage activation by wear particles and metal ions still remain largely unknown. Murine BMDM were used in this study because of their superior physiological relevance to *in vivo* systems compared to mutagenic cell lines (209). In addition, they provide a higher yield per mouse and are easier to generate compared to other sources of primary murine macrophages such as peritoneal or alveolar macrophages (210–212). Finally, besides being the macrophage model of choice in most immunological studies (212), BMDM have been previously used to investigate Ni^{2+}-induced inflammasome activation (172).

Results revealed a concentration-dependent increase in BMDM mortality with the three ions analyzed. Overall, Co^{2+} and Ni^{2+} were more toxic than Cr^{3+}, which corroborate previous studies

with J774 macrophages (94,192). The presence of the different inhibitors (Z-WEHD-FMK, L-ascorbic acid, JSH-23) had minimal toxic effect at the concentrations analyzed (see Supporting Information).

Results also showed an ion concentration-dependent increase in IL-1β release with Cr^{3+} and with Ni^{2+} (albeit to a lower extent), while Co^{2+} had only limited or non-significant effects. Indeed, while the results of the experiments analyzing the effects of caspase-1 inhibitor showed a small but statistically significant IL-1β increase with Co^{2+} (up to 64%), the release was not significant when analyzing the effects of L-AA, revealing an inter-animal variability (100% of the animals responded positively to Cr^{3+} and Ni^{2+} whereas less than 50% of the animals responded positively to Co^{2+}), and the fact that the small increase that was initially observed was not biologically significant. Interestingly, IL-1β release was the highest with Cr^{3+} (almost 5 times higher than with Ni^{2+}) and was inhibited by the presence of Z-WEHD-FMK, a cell-permeabilized fluoromethyl ketone (FMK)-derivatized peptide acting as a specific inhibitor of caspase-1. This strongly suggests that IL-1β release was dependent on pro-IL-1β cleavage by caspase-1. Because caspase-1 catalytically auto-activates when assembled by the NLRP3 inflammasome complex (23,139,145), results point to Cr^{3+} being an activator of the inflammasome. The much lower IL-1β release with Ni^{2+}, together with the absence of active caspase-1 by western blotting (possibly because of signal below detection limit), suggests that Cr^{3+} is a more potent activator of the NLRP3 inflammasome than Ni^{2+}. In addition, while the level of IL-1β with Ni^{2+} in the presence of caspase-1 inhibitor was not statistically different from that in the negative control (likely because of the relatively large S.E.M.), it remained at 174% and 146% of the negative control with 48 ppm and 72 ppm Ni^{2+}, respectively, suggesting that the inhibition of IL-1β by the caspase-1 inhibitor might not be complete and that Ni^{2+} may therefore be acting through additional molecular mechanisms. Finally, Co^{2+} appeared to have limited or non-significant effects on the inflammasome pathway.

Interestingly, past studies have shown that the three metal ions analyzed in the present study induce IL-1β release and point to NLRP3 inflammasome activation as the most probable cause (18,19,172). For example, Caicedo et al. (18,19) showed that Co^{2+}, Cr^{3+}, and Ni^{2+} led to IL-1β release in isolated primary human macrophages, and that this release was caspase-1- and NLRP3 inflammasome-dependent. Of note is that the authors reported levels of IL-1β that were

significantly higher than the ones observed in the present study, which may be explained by differences in cell types (human vs. murine), and/or differences in experimental design. Additionally, Li et al. (172) reported that Ni^{2+} induces IL-1β release via the NLRP3 inflammasome pathway in different cell types, including BMDM. The levels of IL-1β with BMDM were the lowest, but were overall comparable to those with Ni^{2+} in the present study using the same cells. Interestingly, while Li et al. also demonstrated the presence of the active caspase-1 subunit (p20) in lysates of phorbol 12-myristate 13-acetate (PMA)-primed THP-1 cells exposed to an equivalent of 90 ppm Ni^{2+} (suggesting inflammasome activation), p20 was not detected in the supernatants of BMDM exposed to 48 ppm Ni^{2+} in the present study. The differences in the Ni^{2+} concentrations are unlikely to explain the differences in the p20 subunit detection, since IL-1β release was significantly lower with 96 ppm Ni^{2+} than with 48 ppm in the present study. However, once again, differences in cell types (immortalized human cells in Li et al. study vs. primary BMDM in the present study), and/or differences in experimental design may explain the differences in the results. Of note is that culture supernatants were analyzed in the present study since the bulk of stably active caspase-1 has been reported to be secreted following inflammasome activation (147,213). Assuming that the inflammasome is assembled in BMDM in response to Ni^{2+} (as suggested by the detection of IL-1β, albeit at lower levels than with Cr^{3+}), it is possible that the absence of the p20 subunit detection by western blotting may have been due to a signal below the detection threshold. Finally, some studies (11,124) reported no IL-1β release by THP-1 cells in response to Co^{2+} and Cr^{3+}. While results with Co^{2+} corroborate those from the present study, differences with Cr^{3+} may be explained by differences in the ion concentration (higher in the present study). Overall, the reported levels of IL-1β release are highly variable across studies, likely due to differences in cell types, cell culture reagents, and even methodologies, including ion solution preparation.

The NLRP3 inflammasome has been shown to be activated by a wide array of danger patterns, including pathogen-derived proteins (140), inorganic silica crystals, and aluminum salts (142,144,214). Indeed, the NLRP3 inflammasome has been identified as a potential sensor of metabolic danger or stress (215). Because of the significant structural differences between these activators, the NLRP3 inflammasome is not thought to bind directly to its activators or be dependent on a single activation pathway (23). Instead, NLRP3 inflammasome activation is thought to be the result of potentially concomitant signaling pathways, including ROS

production (216), K^+ efflux, lysosomal rupture, and/or spatial rearrangement of organelles (23,114). Studies have shown that Cr^{3+} lead to the production of ROS such as superoxide ions, hydrogen peroxide, and hydroxyl radicals via redox cycling (191). Additionally, metal ions may be causing a dysfunction of the mitochondria, which are responsible for most ROS production (23). It has also been previously demonstrated that metal ion-induced inflammasome activation was dependent on nicotinamide adenine dinucleotide phosphate (NADPH)-generated ROS in THP-1 cells (18). It is therefore possible that metal ions induce inflammasome activation via ROS production. Remarkably, results of the present study showed that the presence of L-AA, an inhibitor of ROS production, inhibited caspase-1 activation (no detection of p20 subunit) as well as IL-1β release in BMDM exposed to Cr^{3+}, suggesting the involvement of ROS in Cr^{3+}-induced inflammasome activation and subsequent production of active caspase-1.

To determine the role of the NF-κB pathway in Cr^{3+}-induced inflammasome activation, BMDM were cultured in presence of JSH-23 during the priming incubation (LPS exposure), activation incubation (ion exposure), or both. JSH-23 is an inhibitor of the NF-κB transcription factor, and unlike most NF-κB inhibitors, which act by preventing IKK (IκB kinase) from degrading IκBα (inhibitor of NF-κB alpha) and releasing active NF-κB, JSH-23 acts by preventing nuclear translocation of active NF-κB (217). It is well established that inflammasome priming relies on the NF-κB pathway (23,107,114,139,146), and Bauernfeind et al. (107) reported that NLRP3 induction (priming) and caspase-1 activation were dose-dependently inhibited by an NF-κB inhibitor (Bay11-7082) in C57BL/6J immortalized wild-type splenic macrophages. Interestingly, results in the present study showed that the presence of 60 μM JSH-23 during the priming incubation only partially reduced Cr^{3+}-induced IL-1β release, while 30 μM of JSH-23 completely blocked the expression of pro-IL-1β transcripts in RAW 264.7 exposed to LPS (217). The effects of JSH-23 concentrations higher than 60 μM were not tested in the present study due to cytotoxicity concerns. It is possible that the partial, as opposed to complete, inhibition of IL-1β may have been due to residual LPS remaining during the activation incubation (when JSH-23 was not present), which may have induced some priming. Indeed, despite the removal of LPS-containing media and rinsing of the cells prior to ion exposure, residual LPS may have remained on cell membranes and culture substrate surfaces.

Surprisingly, the presence of JSH-23 during exclusively the activation incubation (with the ions) partially decreased Cr^{3+}-induced IL-1β release, suggesting a role for NF-κB specifically during the activation of the inflammasome. While NLRP3 inflammasome activation has been reported to have regulatory effects on NF-κB activation (218), the regulation of NLRP3 activation by NF-κB remains largely unknown. In the present study, the role of NF-κB during the activation may have been related to residual LPS from the priming incubation, prolonging the production of NLRP3 and pro-IL-1β past the priming incubation. The presence of JSH-23 during the activation incubation would then suppress this prolonged production of NLPR3 and pro-IL-1β, thereby decreasing mature IL-1β release. Nevertheless, the potential effects of NF-κB on the inflammasome activation cannot be excluded. Interestingly, the presence of JSH-23 throughout both the inflammasome priming and activation incubations led to a significant decrease in Cr^{3+}-induced IL-1β release, down to levels similar to those in the negative control (cells with no ions and no JSH-23). This suggests that metal ion-induced inflammasome assembly is dependent on the NF-κB pathway, though the relative involvement of this pathway during the priming and activation incubations remains to be further investigated.

Of note is that priming of the BMDM with LPS prior to metal ion exposure was necessary to detect IL-1β release, which is in agreement with the *in vitro* model of macrophage priming with a TLR4 ligand (151,152). Greenfield et al. (157,158) also demonstrated that endotoxins adherent to titanium particles greatly enhanced the particle biological activity via TLR2 and TLR4 binding in both RAW 264.7 macrophages and BMDM, and suggested that endogenous alarmins caused by particle-induced damage are not sufficient to activate TLR. Furthermore, Samelko et al. (113) recently reported that the IL-1β release by murine peritoneal macrophages exposed to CoCr particles more than doubled when LPS (a TLR-4 ligand) was present. However, in contrast with the present study, the addition of LPS was not necessary to observe IL-1β release. This difference may be due to differences in cell types (peritoneal macrophages in Samelko et al. vs. BMDM in the present study), or due to potential differences in the FBS used in the culture medium (undisclosed grade of FBS in Samelko et al. vs. ultra-low endotoxin FBS in the present study). In any case, it should be noted that *in vivo*, priming may also be achieved by endogenous factors or alarmins (219–221), by ions directly binding to a (human) TLR or through PAMP (including LPS) originating from a subclinical bacterial biofilm on the implant material surface (50,111).

In conclusion, this study demonstrated that Cr^{3+} and Ni^{2+} induced IL-1β release (probable indicator of inflammasome assembly) by BMDM. Nevertheless, the much higher release of IL-1β with Cr^{3+} and the absence of detectable active caspase-1 subunit with Ni^{2+} suggest that Cr^{3+} is a more potent activator of this pathway. Co^{2+}, on the other hand, appeared to have either limited or non-significant effects on the activation of this pathway. Finally, results showed that caspase-1 activation with Cr^{3+} was oxidative stress-dependent, and that the NF-κB pathway was involved in IL-1β release. Overall, this study provides insights into the mechanisms of metal ion-induced NLRP3 inflammasome activation in macrophages, which may eventually help the development of pharmaceutical approaches to modulate the inflammatory response to metal ions, and thereby increase implant longevity.

4.7 Acknowledgements

The authors thank Dr. Julie Joseph and Norah A. Alturki for expert advice on BMDM preparation, Emily Ertel and Hallie Arnott for data collection, as well as Dr. Eric Lehoux, Kriti Kumar, and Jennifer Ham for technical assistance. This work was supported by the Canadian Institutes of Health Research (CIHR), the Canada Research Chairs (CRC) Program, and the Ontario Ministry of Research and Innovation (MRI) (I.C.).

4.8 Supplementary Information

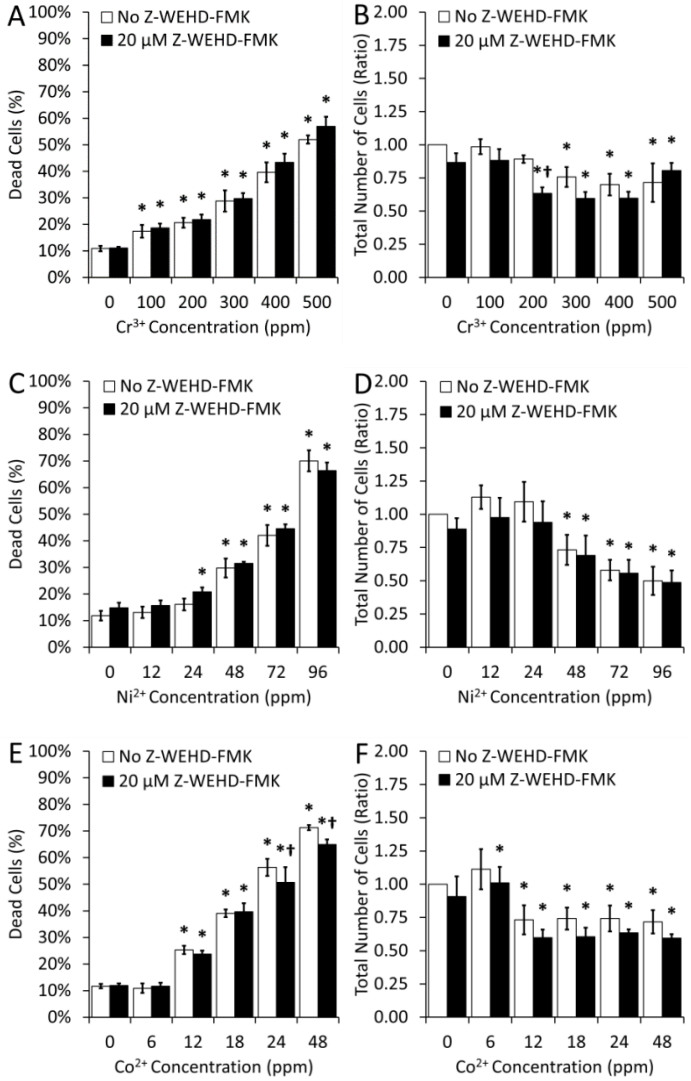

Supplementary Figure 1. Mortality of bone marrow-derived macrophages (BMDM) after exposure to Cr^{3+}, Ni^{2+}, or Co^{2+}, with or without Z-WEHD-FMK: (A, C and E) Percentages of dead cells; (B, D and F) Total numbers of cells (viable and dead). Cells were incubated with the indicated concentrations of ions with or without 20 µM Z-WEHD-FMK (caspase-1 inhibitor) for 18 to 24h under cell culture conditions after a 6h priming incubation with 500 ng/mL of lipopolysaccharide (LPS). Cells were counted by hemocytometry and dead cells were identified using the trypan blue dye-exclusion method. The total numbers of cells (viable and dead) were expressed as a ratio of the total number of cells in the negative control (cells with no ions and no Z-WEHD-FMK). An asterisk (*) indicates a significant difference ($p<0.05$) between a given ion concentration with or without Z-WEHD-FMK and the negative control. A dagger (†) indicates a difference ($p<0.05$) between a given ion concentration with Z-WEHD-FMK and the same ion concentration without Z-WEHD-FMK. Data are presented as means ± SEM of 3-4 independent experiments performed in triplicate.

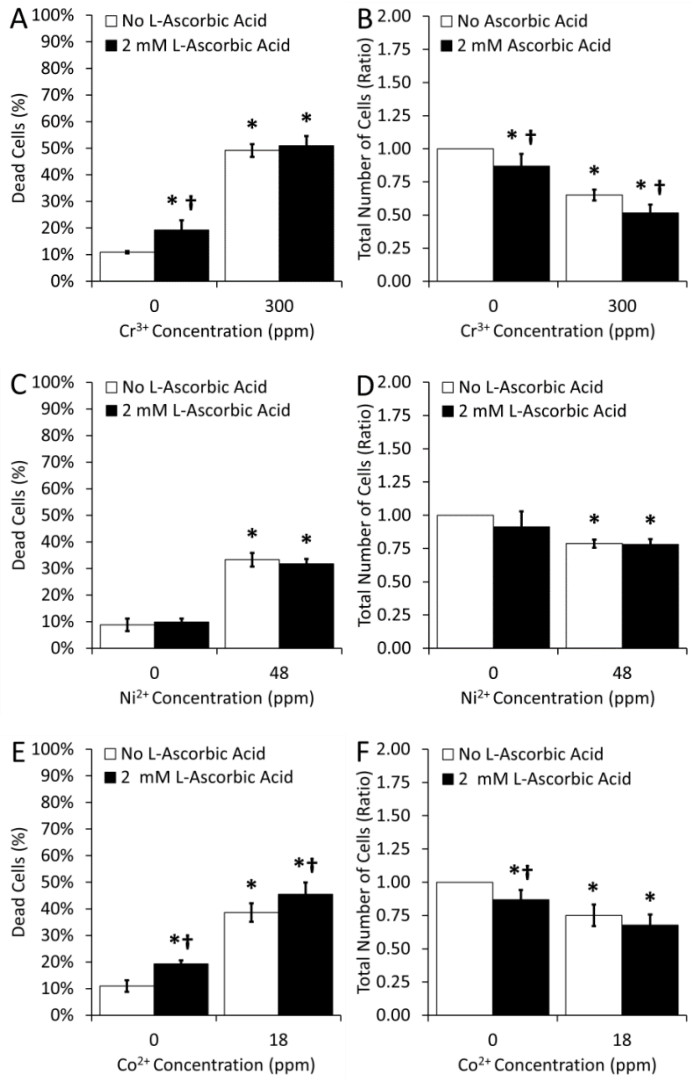

Supplementary Figure 2. Mortality of bone marrow-derived macrophages (BMDM) after exposure to Cr^{3+}, Ni^{2+}, or Co^{2+}, with or without L-AA: (A, C and E) Percentages of dead cells; (B, D and F) Total numbers of cells (viable and dead). Cells were incubated with the indicated concentrations of ions with or without 2 mM L-AA (oxidative stress inhibitor) for 18 to 24h under cell culture conditions after a 6h priming incubation with 500 ng/mL of lipopolysaccharide (LPS). Cells were counted by hemocytometry and dead cells were identified using the trypan blue dye-exclusion method. The total numbers of cells (viable and dead) were expressed as a ratio of the total number of cells in the negative control (cells with no ions and no L-AA). An asterisk (*) indicates a significant difference ($p<0.05$) between a given ion concentration with or without L-AA and the negative control. A dagger (†) indicates a difference ($p<0.05$) between a given ion concentration with L-AA and the same ion concentration without L-AA. Data are presented as means ± SEM of 3 independent experiments performed in triplicate.

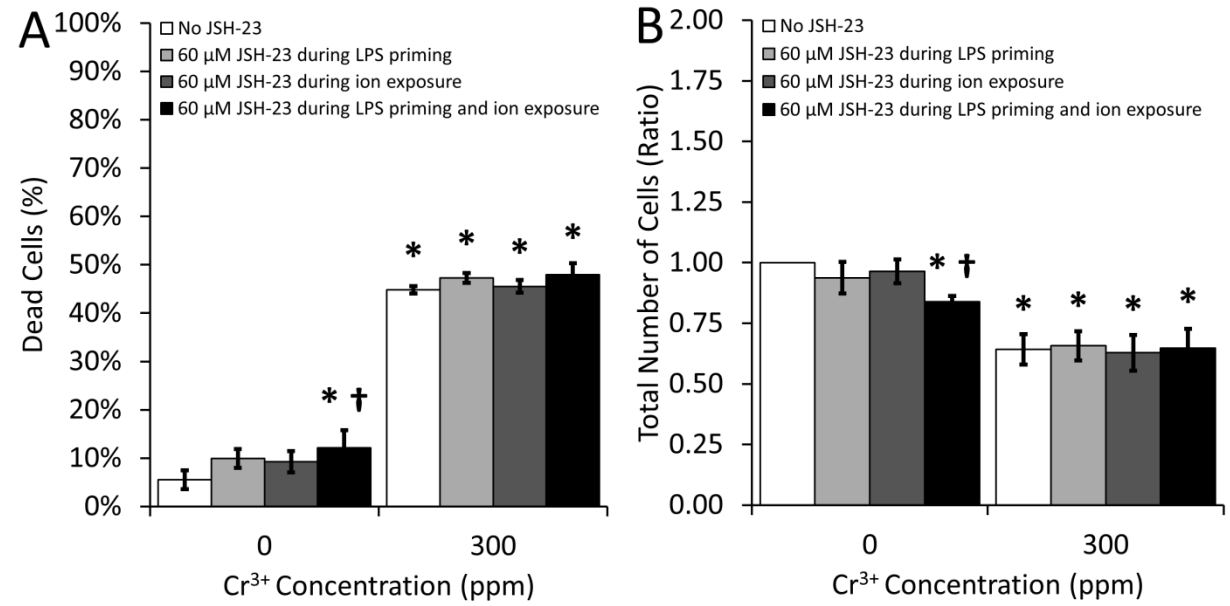

Supplementary Figure 3. Mortality of bone marrow-derived macrophages (BMDM) after exposure to Cr^{3+} with or without JSH-23: (A) Percentages of dead cells; (B) Total numbers of cells (viable and dead). Cells were incubated with 0 or 300 ppm Cr^{3+} for 18 to 24h with or without 60 µM JSH-23 (NF-κB inhibitor) under cell culture conditions after a 6h priming incubation with 500 ng/mL of lipopolysaccharide (LPS). In total, four JSH-23 conditions were tested: no JSH-23 (white bars), JSH-23 present exclusively during the priming incubation with LPS (light gray bars), JSH-23 present exclusively during the activation incubation with Cr^{3+} ions (dark gray bars), and JSH-23 present during both incubations (black bars). An asterisk (*) indicates a significant difference ($p<0.05$) between a given ion concentration with or without JSH-23 and the negative control (cells with no ions and no JSH-23). A dagger (†) indicates a significant difference ($p<0.05$) between a given ion concentration with JSH-23 and the same concentration without JSH-23. Data are presented as means ± SEM of 3 independent experiments performed in triplicate.

5 Thesis Discussion

5.1 Conclusions from the Work

This thesis examined some of the key molecular mechanisms involved in the inflammatory response to metal ions from implantable biomaterials. Specifically, the response of macrophages to cobalt(II), chromium(III), and nickel(II) ions was analyzed in terms of caspase-1 enzyme activation (necessary for mature IL-1β production) and pro-inflammatory cytokine IL-1β release. Results presented in the manuscript also include the analysis of the potential involvement of oxidative stress and the NF-κB signaling pathway. The results presented in the manuscript fulfill the three objectives of this thesis, which were to: 1) determine if, in macrophages, IL-1β release induced by Co^{2+}, Cr^{3+}, or Ni^{2+} is caspase-1-dependent; 2. determine if, in macrophages, caspase-1 activation and IL-1β release induced by Co^{2+}, Cr^{3+}, or Ni^{2+} are oxidative stress-dependent; and 3. determine if, in macrophages, IL-1β release induced by Co^{2+}, Cr^{3+}, or Ni^{2+} is NF-κB signaling pathway-dependent.

To fulfill the first objective, BMDM were exposed to various concentrations of Co^{2+}, Cr^{3+}, or Ni^{2+} in the presence or absence of Z-WEHD-FMK, a specific caspase-1 inhibitor. Results showed that Cr^{3+} induced the highest release of IL-1β, while Co^{2+} had limited or non-significant effects. The addition of Z-WEHD-FMK induced a decrease in IL-1β release with all three ions, down to or below the level of the negative control, suggesting IL-1β release was dependent on caspase-1.

To fulfill the second objective, BMDM were exposed to 18 ppm Co^{2+}, 300 ppm Cr^{3+}, or 48 ppm Ni^{2+} (concentrations that were shown to induce the highest IL-1β release for each ion in objective 1) in the absence or presence of L-AA, an inhibitor of oxidative stress. Immunoblotting revealed the presence of the cleaved active caspase-1 p20 subunit in supernatants of BMDM incubated with Cr^{3+}, but not with Ni^{2+} or Co^{2+}. When L-AA was present with Cr^{3+}, the cleaved subunit was undetectable and IL-1β release decreased down to the level of the negative control, demonstrating that caspase-1 activation and IL-1β release induced by Cr^{3+} was oxidative stress-dependent. The addition of L-AA also led to a decrease in IL-1β release with Ni^{2+} (below the level of the negative control), suggesting that IL-1β release induced by Ni^{2+} was also oxidative stress-dependent. Co^{2+} did not induce significant IL-1β release.

To fulfill the third and final objective, BMDM were exposed to 300 ppm Cr^{3+} (the ion and the concentration that were shown to induce the highest IL-1β release, and the only ion that was shown to induce detectable active caspase-1 in objective 1) in the absence or presence of JSH-23, an inhibitor of the NF-κB signaling pathway. Results revealed that JSH-23 blocked Cr^{3+}-induced IL-1β release, but only if present during both the priming incubation with LPS (also known as "signal 1" in the inflammasome literature) and the activation incubation ("signal 2") with ions. These results suggest that Cr^{3+}-induced IL-1β release is dependent on the NF-κB signaling pathway, and that NF-κB may play a role during both the priming and activation of the inflammasome.

These findings bring new insights into the molecular mechanisms involved in the macrophage response to metal ions. Continued research efforts along this path may lead to a more complete understanding of the pathogenesis of aseptic loosening, which may eventually uncover new avenues of modulation or prevention of the inflammatory response responsible for implant loosening.

5.2 Technical Considerations

5.2.1 Optimization of Bone Marrow-Derived Macrophage Generation

The present research project used BMDM as a model for *in vitro* cell culture work. As such, it was critical to optimize their generation for both quality and quantity. The mouse dissection and bone marrow flushing protocol was adapted from the thesis of S. McComb, a former Ph.D. student in Dr. Sad's laboratory at the University of Ottawa. The bone marrow precursor cell plating and differentiation protocol was finalized after optimizing the following parameters: the M-CSF concentration, the seeding density of bone marrow precursor cells, the type of cell culture dish used for the culture of precursor cells, and the detachment method of mature BMDM.

M-CSF was used to differentiate the precursor cells since it is known to induce hematopoietic precursor cell differentiation into mature BMDM (222). Since M-CSF is secreted by L-929 cells, L-929 cell culture supernatant can be added to bone marrow precursor cell differentiation media to induce macrophage differentiation (222). However, the use of L-929 cells has several drawbacks, such as variations in M-CSF concentration from batch-to-batch, and the need to maintain large volumes of L-929 cell cultures while minimizing contamination risks. More

recently, recombinant M-CSF (rM-CSF) has become commercially available (223), and it is increasingly being used in place of L-929 culture supernatant. rM-CSF can be added to precursor cell media at precise concentrations (224), and significantly simplifies lab procedures while reducing overall costs. As such, rM-CSF was chosen as the differentiation agent for the present research project. Three rM-CSF concentrations (5, 10, and 20 ng/ml) were tested based on previously published BMDM generation protocols (210,211,222,223,225,226). The optimal precursor cell seeding density had to be determined in tandem with the optimal rM-CSF concentration, since these two parameters can influence each other. Indeed, higher seeding densities may necessitate higher M-CSF concentrations, as M-CSF is consumed by cells. The tested seeding densities (200,000, 300,000 or 400,000 per cm^2) were based on previously published BMDM generation protocols (210,211,222,223,225,226). It was empirically determined that 5 ng/ml rM-CSF along with a seeding density of 200,000 cells/cm^2 consistently led to a monolayer of BMDM at approximately 80% confluency in standard 100 mm-diameter dishes. Higher M-CSF concentrations or seeding densities were judged to be cost-ineffective.

Finally, two types of dish surface treatments were tested: suspension vs. tissue culture (TC) surfaces. Suspension and TC surfaces are widespread and suitable for many types of cells. It should be noted that several other surface treatments are commercially available, but many of these are specific to a cell type, model, or application. Suspension surfaces are smooth and do not facilitate cell adhesion. As such, they are generally applicable to non-adherent cells (cultured in suspension). Conversely, TC dishes are specially treated to facilitate cell attachment and are thus applicable to the culture of adherent cells. Both surface types yielded comparable numbers of BMDM with similar morphologies, and BMDM formed an adherent monolayer on both surfaces. However, the BMDM could not be easily detached from TC surfaces prior to experimental setup. The optimal dish surface type was therefore determined in tandem with the detachment method, as the surface affects the ease of detachment. Different detachment methods of mature BMDM were tested. Gentle cell scraping in PBS with a disposable beveled-edge cell lifter led to unacceptable high mortality (>10%) from both surface types (suspension and TC). A pre-existing fluid pressure-induced pipette washing detachment method was then tested. This method had been successfully used by Dr. Lehoux (Research Associate in the lab) and Z. Salloum (Ph.D. student in the lab) for RAW 264.7 macrophages and was adapted to BMDM. This method led to high (>10%) mortality with TC surfaces, but consistently yielded acceptable

(<10%) mortality with suspension surfaces. Therefore, suspension surfaces were used for BMDM differentiation for the remainder of the research project, and BMDM were always detached with the pipette washing method. The table below summarizes the tested parameters and optimal selections:

Table 1: Optimization of parameters for BMDM generation

Parameter	***Test cases***	***Optimal selection***
M-CSF concentration	5, 10, and 20 ng/ml	5 ng/ml
Bone marrow precursor cell seeding density	200,000, 300,000 and 400,000 cells per cm^2 of dish surface	200,000 cells per cm^2 of dish surface
Cell culture dish surface treatment	Suspension or tissue culture-treated	Suspension
Detachment method	Scraping or pipette fluid pressure wash	Pipette fluid pressure wash

5.2.2 Analysis of Macrophage Phenotype by Flow Cytometry

Following the optimization of the BMDM generation protocol, it was necessary to verify the phenotype of the cells. This analysis was performed by flow cytometry. Four surface markers were initially targeted: F4/80, CD11b, CD11c, and Ly6C, as described in Table 2 below, to verify that the precursor cells had been differentiated into macrophages.

Table 2: Markers for flow cytometry

Marker	*Cell type identified*	*References*
F4/80	Murine macrophages	Dos Anjos Cassado et al. (227), Lin et al. (228,229).
CD11b	Myeloid lineage marker	Antonios et al. (230), Rasmussen et al. (231)
CD11c	Generally expressed by murine dendritic cells	Kurts et al. (232), Singh-Jasuja et al. (233)
Ly6C	Immature myeloid cells, monocytes,	Deng et al. (234), Yang et al. (235)

It should be noted that although these markers are useful for cell identification, they are membrane proteins that serve a cellular function. For example, F4/80 is a 160 kDa glycoprotein receptor thought to be involved in immunological induction (236). The desired markers for the BMDM were F4/80+, CD11b+, CD11c-, and Ly6C-. Indeed, this would indicate that the cells are mature murine macrophages, and not dendritic cells (which would be CD11c+) or immature macrophages (which would be LY6C+).

The first analysis revealed that the vast majority of cells were F4/80+, CD11b+, CD11c+, and Ly6C-. The result was unexpected since cells cannot be both macrophages and dendritic. This discrepancy was attributed to a potential technical problem due to the simultaneous use of 4 different fluorochromes with partly overlapping emission spectra (overlaps increase the risk of false positives). Since the cells were all Ly6C-, it was decided to eliminate this marker in subsequent tests, bringing down the number of fluorochromes analyzed to three.

Because macrophages (among other immune cell types) possess Fc (Fragment, crystallizable) receptors on their surface that can bind the Fc region of fluorochrome resulting in false positives, an Fc receptor blocking step (with CD16/CD32 antibody) was added prior to fluorochrome

staining in subsequent analyses. Nevertheless, flow cytometric analysis still revealed a population of cells positive for CD11c. Although CD11c has a history of experimental use as a DC marker, its specificity has recently been questioned (237,238). Therefore, it was then decided to substitute CD11c+ for dendritic cell inhibitory marker 2 (DCIR2), which is marketed as a specific murine dendritic cell marker (239). Unexpectedly, results still revealed a large DCIR2+ cell population. Since it was judged highly improbable that the cells were factually positive for both markers, technical troubleshooting continued.

Although BMDM (and primary macrophages in general) are known to be highly autofluorescent (211), significant batch-to-batch variability across cells from different mice was not initially considered, and a retrospective analysis of flow cytometric results displaying large populations of seemingly CD11c or DCIR2 positive cells revealed an increasing and uncompensated auto-fluorescence in the same wavelength channel (575nm/40) as the expected emissions from CD11c and DCIR2 fluorochromes. Subsequent flow cytometric analyses with careful correction for cell auto-fluorescence during the signal acquisition revealed that the cells were, in fact, F4/80+ and DCIR2-, confirming their macrophage phenotype.

5.2.3 Optimization of the Western Blotting Protocol for the Detection of Active Caspase-1

Western blotting was used to detect the active subunit of the caspase-1 enzyme (p20). The small size of the protein (20 kDa) combined with its dilute presence in cell culture media (supplemented with substantial amounts of serum proteins) created significant technical challenges for reliable protein detection. In order to detect small and in low-abundance proteins in mammalian cell culture media, key parameters to optimize include the gel type, membrane type, protein transfer conditions, choice of primary antibody suppliers, and the imaging system.

Commercial gels were chosen due to the availability of pre-cast polyacrylamide gradient gels. As proteins migrate down a gradient gel, the decreasing gel pore size (a result of increasing polyacrylamide percentage due to the gradient) halts the migration of proteins that are too large to pass through the pores. Important advantages include better separation of proteins with similar molecular weights, and the ability to separate proteins of a wider range of molecular weights (240). These advantages are especially useful for the clean separation of small proteins in low

abundance. Commercial pre-cast gels also offer considerable time savings compared to the preparation of "home-made" gels and improve the consistency of protein separation results.

Significant optimization had to be done with regards to the choice of membrane type, protein transfer conditions (i.e., transfer voltage and time), and choice of primary antibody suppliers. While smaller membrane pore sizes allow for better retention of small proteins, they can also capture more secondary antibody resulting in high background signal during imaging (241). In the present study, high background proved to be a significant obstacle with 0.22-micron pore membranes, forcing the use of 0.45-micron pore membranes, which led to markedly better signal-to-noise ratios. Furthermore, during protein transfer, voltage (and thus electric field force) and transfer time play critical roles in small protein detection. Indeed, low voltages and short transfer times may not transfer detectable amounts of small proteins from the gel to the membrane, while excessive voltage and time may lead to small proteins passing through the membrane instead of being retained. After extensive troubleshooting, the optimum transfer conditions were determined to be at 100 V for 1 hour. Finally, the quality of the primary antibody was found to be extremely important. Initial attempts to detect caspase-1 could only detect the 45 kDa pro-form; the smaller 20 kDa active subunit could not be detected. It was thought that the 20 kDa subunit, if present, was too dilute for reliable detection within the cell culture medium that is supplemented with FBS. Indeed, due to the presence of FBS, a majority of the proteins within the samples are serum proteins such as albumin. A novel albumin-filtering process using urea to denature proteins prior to high-speed centrifugal filtering with commercially available tube filters was therefore tested. Urea was selected among several protein denaturants due to its chemical compatibility with the regenerated cellulose used in the tube filters. Initial results appeared promising, with proteins bands in the 60-kDa range disappearing from post-transfer membranes. However, probing for caspase-1 revealed that both the pro-form and the active form were no longer detectable in albumin-filtered samples. It is possible that the 50-kDa molecular weight cut-off of the tube filters was too close to the molecular weight of pro-caspase-1 (45 kDa), resulting in much of the pro-form being removed from the samples. Filter clogging by large serum proteins or albumin overload could also have accounted for the absence of detectable pro- and active caspase-1. As the albumin-filtering process did not lead to active caspase-1 detection, it was decided that new primary antibodies should be investigated. Ultimately, the active subunit was not detected until the primary antibody

was changed, highlighting the importance of antibody validation studies. Indeed, it has been reported that the field of biomedical sciences is experiencing a reproducibility crisis and that antibodies constitute a large part of the problem (242,243). Additional troubleshooting experiments revealed that albumin-filtering was not necessary with the new primary antibody. Therefore, this additional albumin-removal step was not pursued.

Finally, another important parameter affecting the protein detection using ECL is the imaging system. The first imaging system that was used (GE ImageQuant LAS 4000) was equipped with an unremarkable digital imaging sensor. The use of an advanced system (LICOR Odyssey Fc) with an imaging sensor featuring a much wider dynamic range allowed for improved detection of faint active caspase-1 bands, resulting in higher quality blot images. While ECL allowed for the fulfillment of the thesis objectives, the signal-to-noise ratio could have possibly been further improved with the use of fluorescence imaging instead of chemiluminescence imaging, since fluorochromes exhibit better sensitivity and signal stability. First described in the late 1990s, fluorescent detection methods have recently been gaining in popularity as reagent costs decrease and general-purpose protocols are disseminated (244). It is speculated that fluorescent detection may eventually overtake ECL as the most common western blot imaging technique, just as ECL overtook earlier radioactive and colorimetric detection methods (244).

5.3 Future Studies

5.3.1 Inclusion of Additional Metal Ions and Metal Particles

The present research project focused on the effects of Co^{2+}, Cr^{3+}, and Ni^{2+}. However, other metal ions may also be involved in the inflammatory response to metal implants. For example, although molybdenum ion release by CoCrMo alloy is much lower compared to cobalt and chromium ions (245), molybdenum ions could be considered in future studies since Mo^{5+} has previously been shown to activate the inflammasome in THP-1 cells (18). Since titanium is the principal element in the widespread TiAl6V4 alloy used in many orthopaedic implant components, titanium ions may also be considered. The thesis project originally included titanium ions, specifically Ti^{4+}. However, titanium chlorides are highly toxic and reactive. Indeed, $TiCl_4$ is a highly volatile metal halide that can react with humid air to form HCl (246). The inclusion of titanium ions would possibly necessitate the use of plasma standard solutions, which contain acid to stabilize the metal in an ionic form. These solutions must be handled with

care as they can cause severe skin burns. Finally, metal particles of different sizes and shapes may also be included in future studies. CoCrMo particles, for example, have been shown to activate the inflammasome (112).

5.3.2 Measurement of Intracellular Reactive Oxygen Species

Previous studies have shown that ROS can induce the activation of the inflammasome (23,114,182,188). Interestingly, an important finding of this thesis was that L-AA (a ROS scavenger) successfully prevented caspase-1 activation and IL-1β release in macrophages exposed to Cr^{3+}. Both caspase-1 activation and IL-1β release are expected downstream of inflammasome activation. Therefore, the findings suggest that L-AA is scavenging Cr^{3+}-induced ROS that would possibly otherwise activate the inflammasome. This would need to be confirmed by intracellular ROS measurements. Such measurements may also provide some insight as to why Co^{2+} and Ni^{2+} induced much lower levels of IL-1β release with no detectable amounts of active caspase-1. For instance, it may be found that Co^{2+} and Ni^{2+} induce less oxidative stress in BMDM than Cr^{3+}.

5.3.3 Examination of Inflammasome Component Proteins

A limitation of the present research project is that inflammasome component proteins (NLRP3 and ASC) were not analyzed. Instead, the analysis focused on proteins that are expected downstream of inflammasome activation (caspase-1 and IL-1β). Therefore, NLRP3 and ASC should be analyzed to confirm inflammasome activation in future studies.

The NLRP3 inflammasome is thought to be an intracellular signaling platform, and therefore, component proteins such as NRLP3 and ASC may be detectable in cell lysates by western blot. Interestingly, it has also been reported that the inflammasome may be secreted upon activation, although the physiological purpose is unclear, beyond enabling the cleavage of pro-caspase-1 in the extracellular space (148). It should be noted that the extracellular space may contain inflammasome proteins as well as pro-forms of inflammatory cytokines and enzymes due to cells releasing their contents following necrosis. Supernatants should therefore also be considered in conjunction with lysates in future studies.

Gene knock-down technologies may also be considered as an alternative to western blot. Gene knock-down forms the basis of functional genetic studies that seek to investigate the function of specific genes (247). In the context of the inflammatory response to orthopaedic wear products,

selectively silencing genes that code for inflammasome components and monitoring the inflammatory response may yield valuable mechanistic insight. For example, it may reveal that certain proteins are dispensable to the inflammatory process, or that others are good candidates for pharmaceutical modulation. Gene knock-down in cells of interest may be achieved in a number of ways. A commonly used method in *in vitro* studies is RNA interference (RNAi). RNAi technologies transfect cells with small interfering RNA (siRNA) designed to bind and interfere mRNA, preventing their translation into proteins (248–250). For this reason, RNAi is also known as post-transcriptional gene silencing. Important drawbacks of RNAi techniques include difficulties with cell transfection, incomplete or very short-lived gene knock-down, and costs (251).

5.3.4 In Vivo Model of Osteolysis

The present research project used an *in vitro* macrophage culture system, wherein primary murine macrophages were cultured in isolation and in the presence of antibiotics. Compared to an *in vivo* model, *in vitro* models possess some notable advantages. For example, they allow for a detailed study of a specific mechanism within a cell type, such as the caspase-1 and IL-1β activation mechanisms, which were analyzed in the present work. They also serve to control costs and allow for a greater number of experiments. However, the results of *in vitro* studies can hardly be extrapolated to correctly predict the response of a whole complex organism (252). Indeed, considerable effort continues to be expended to refine extrapolation techniques, especially in the field of pharmacology where risks of drug-drug interactions must be continually and rapidly assessed. All things considered, the ability of metal ions to induce IL-1β release (or any other inflammatory cytokine) in macrophages *in vitro* may not directly translate to metal ion-induced osteolysis or other problems *in vivo*. Nevertheless, it must be noted that *in vitro* studies are a necessary step before *in vivo* studies and the results of *in vitro* studies inform the design of *in vivo* experiments.

To better understand the role that metal ions and other wear or corrosion products play in problems of clinical relevance such as periprosthetic osteolysis or other adverse tissue reactions, *in vivo* models must be considered. Two murine models have been primarily used for the study of the inflammatory response generated by wear products: the calvaria osteolysis model (113,253) and the air pouch model (5,254–257). *In vivo* models, informed by the results of

targeted *in vitro* studies, may help determine to what extent the inflammasome is involved in clinical problems.

6 References

1. Chen Q, Thouas GA. Metallic implant biomaterials. Mater Sci Eng R Rep. 2015 Jan 1;87(Supplement C):1–57.

2. Breme H, Biehl V, Reger N, Gawalt E. Chapter 1a Metallic biomaterials: introduction. In: Handbook of Biomaterial Properties [Internet]. Springer, New York, NY; 2016 [cited 2017 Nov 27]. p. 151–8. Available from: https://link.springer.com/chapter/10.1007/978-1-4939-3305-1_14

3. Saini M, Singh Y, Arora P, Arora V, Jain K. Implant biomaterials: A comprehensive review. World J Clin Cases WJCC. 2015 Jan 16;3(1):52–7.

4. Cadosch D, Chan E, Gautschi OP, Filgueira L. Metal is not inert: Role of metal ions released by biocorrosion in aseptic loosening—Current concepts. J Biomed Mater Res A. 2009 Dec 15;91A(4):1252–62.

5. Afolaranmi GA, Akbar M, Brewer J, Grant MH. Distribution of metal released from cobalt-chromium alloy orthopaedic wear particles implanted into air pouches in mice. J Biomed Mater Res A. 2012 Jun;100(6):1529–38.

6. Andrews RE, Shah KM, Wilkinson JM, Gartland A. Effects of cobalt and chromium ions at clinically equivalent concentrations after metal-on-metal hip replacement on human osteoblasts and osteoclasts: implications for skeletal health. Bone. 2011 Oct;49(4):717–23.

7. Cooper HJ. The local effects of metal corrosion in total hip arthroplasty. Orthop Clin North Am. 2014 Jan 1;45(1):9–18.

8. Man K, Jiang L-H, Foster R, Yang XB. Immunological responses to total hip arthroplasty. J Funct Biomater. 2017 Aug 1;8(3).

9. Goodman SB. Wear particles, periprosthetic osteolysis and the immune system. Biomaterials. 2007 Dec 1;28(34):5044–8.

10. Abu-Amer Y, Darwech I, Clohisy JC. Aseptic loosening of total joint replacements: mechanisms underlying osteolysis and potential therapies. Arthritis Res Ther. 2007;9 Suppl 1:S6.

11. Pettersson M, Kelk P, Belibasakis GN, Bylund D, Molin Thorén M, Johansson A. Titanium ions form particles that activate and execute interleukin-1β release from lipopolysaccharide-primed macrophages. J Periodontal Res. 2017 Feb 1;52(1):21–32.

12. Pandit H, Glyn-Jones S, McLardy-Smith P, Gundle R, Whitwell D, Gibbons CLM, et al. Pseudotumours associated with metal-on-metal hip resurfacings. J Bone Joint Surg Br. 2008 Jul;90(7):847–51.

13. Gill IPS, Webb J, Sloan K, Beaver RJ. Corrosion at the neck-stem junction as a cause of metal ion release and pseudotumour formation. J Bone Jt Surg Br. 2012 Jul 1;94–B(7):895–900.

14. Davis DL, Morrison JJ. Hip arthroplasty pseudotumors: Pathogenesis, imaging, and clinical decision making. J Clin Imaging Sci [Internet]. 2016 Apr 29 [cited 2017 Oct 30];6. Available from: https://www.ncbi.nlm.nih.gov/pmc/articles/PMC4863402/

15. Lawrence H, Deehan D, Holland J, Kirby J, Tyson-Capper A. The immunobiology of cobalt: demonstration of a potential aetiology for inflammatory pseudotumours after metal-on-metal replacement of the hip. Bone Jt J. 2014 Sep;96–B(9):1172–7.

16. Wawrzynski J, Gil JA, Goodman AD, Waryasz GR. Hypersensitivity to orthopedic implants: A review of the literature. Rheumatol Ther. 2017 Jun;4(1):45–56.

17. Teo WZW, Schalock PC. Metal hypersensitivity reactions to orthopedic implants. Dermatol Ther. 2016 Dec 19;7(1):53–64.

18. Caicedo MS, Desai R, McAllister K, Reddy A, Jacobs JJ, Hallab NJ. Soluble and particulate Co-Cr-Mo alloy implant metals activate the inflammasome danger signaling pathway in human macrophages: A novel mechanism for implant debris reactivity. J Orthop Res. 2009 Jul 1;27(7):847–54.

19. Caicedo MS, Pennekamp PH, McAllister K, Jacobs JJ, Hallab NJ. Soluble ions more than particulate cobalt-alloy implant debris induce monocyte costimulatory molecule expression and release of proinflammatory cytokines critical to metal-induced lymphocyte reactivity. J Biomed Mater Res A. 2010 Jun 15;93A(4):1312–21.

20. Fiorito S, Magrini L, Goalard C. Pro-inflammatory and anti-inflammatory circulating cytokines and periprosthetic osteolysis. J Bone Joint Surg Br. 2003 Nov;85(8):1202–6.

21. Stea S, Visentin M, Granchi D, Ciapetti G, Donati ME, Sudanese A, et al. Cytokines and osteolysis around total hip prostheses. Cytokine. 2000 Oct 1;12(10):1575–9.

22. Burton L, Paget D, Binder NB, Bohnert K, Nestor BJ, Sculco TP, et al. Orthopedic wear debris mediated inflammatory osteolysis is mediated in part by NALP3 inflammasome activation. J Orthop Res. 2013 Jan 1;31(1):73–80.

23. Jo E-K, Kim JK, Shin D-M, Sasakawa C. Molecular mechanisms regulating NLRP3 inflammasome activation. Cell Mol Immunol. 2016 Mar;13(2):148–59.

24. Niki Y, Matsumoto H, Suda Y, Otani T, Fujikawa K, Toyama Y, et al. Metal ions induce bone-resorbing cytokine production through the redox pathway in synoviocytes and bone marrow macrophages. Biomaterials. 2003 Apr;24(8):1447–57.

25. Petit A, Mwale F, Tkaczyk C, Antoniou J, Zukor DJ, Huk OL. Induction of protein oxidation by cobalt and chromium ions in human U937 macrophages. Biomaterials. 2005 Jul;26(21):4416–22.

26. Bergmann C, Stumpf A. Biomaterials. In: Dental Ceramics: Microstructure, Properties, and Degradation [Internet]. 1st ed. Springer-Verlag Berlin Heidelberg; 2013. Available from: http://www.springer.com/gp/book/9783642382239

27. Daigle ME, Weinstein AM, Katz JN, Losina E. The cost-effectiveness of total joint arthroplasty: a systematic review of published literature. Best Pract Res Clin Rheumatol [Internet]. 2012 Oct [cited 2017 Oct 29];26(5). Available from: https://www.ncbi.nlm.nih.gov/pmc/articles/PMC3879923/

28. Total joint replacement-OrthoInfo [Internet]. American Academy of Orthopaedic Surgeons. 2014 [cited 2017 Oct 29]. Available from: http://orthoinfo.aaos.org/topic.cfm?topic=a00233

29. Inpatient hospitalizations, surgeries, newborn and childbirth indicators, 2015-2016 [Internet]. Canadian Institute for Health Information; 2017 Apr [cited 2017 Sep 2]. Available from: https://secure.cihi.ca/free_products/cad_hospitalization_and_childbirth_snapshot_2015-2016_en.pdf

30. Ulrich SD, Seyler TM, Bennett D, Delanois RE, Saleh KJ, Thongtrangan I, et al. Total hip arthroplasties: What are the reasons for revision? Int Orthop. 2008 Oct;32(5):597–604.

31. Madeti BK, Chalamalasetti SR, Pragada SKS siva rao B. Biomechanics of knee joint — A review. Front Mech Eng. 2015 Jun 1;10(2):176–86.

32. Bowman KF, Fox J, Sekiya JK. A clinically relevant review of hip biomechanics. Arthroscopy. 2010 Aug;26(8):1118–29.

33. Sophia Fox AJ, Bedi A, Rodeo SA. The basic science of articular cartilage. Sports Health. 2009 Nov;1(6):461–8.

34. Jay GD, Waller KA. The biology of Lubricin: Near frictionless joint motion. Matrix Biol. 2014 Oct 1;39(Supplement C):17–24.

35. Alvarez KE. Total hip replacement. In: New Materials and Technologies for Healthcare. 1st ed. 179-190: Imperial College Press; 2011.

36. Charnley J. The long-term results of low-friction arthroplasty of the hip performed as a primary intervention. J Bone Joint Surg Br. 1972 Feb;54(1):61–76.

37. Cordova LA, Stresing V, Gobin B, Rosset P, Passuti N, Gouin F, et al. Orthopaedic implant failure: aseptic implant loosening–the contribution and future challenges of mouse models in translational research. Clin Sci. 2014 Sep 1;127(5):277–93.

38. Cherian JJ, Jauregui JJ, Banerjee S, Pierce T, Mont MA. What host factors affect aseptic loosening after THA and TKA? Clin Orthop. 2015 Aug;473(8):2700–9.

39. Hip and knee replacements in Canada, 2014-2015 [Internet]. Canadian Institute for Health Information; 2017 Mar. (Canadian Joint Replacement Registry Annual Report). Available from: https://secure.cihi.ca/free_products/cjrr-annual-report-2016-en.pdf

40. Goodman SB, Gibon E, Yao Z. The basic science of periprosthetic osteolysis. Instr Course Lect. 2013;62:201–6.

41. Bougherara H, Zdero R, Shah S, Miric M, Papini M, Zalzal P, et al. A biomechanical assessment of modular and monoblock revision hip implants using FE analysis and strain gage measurements. J Orthop Surg. 2010 May 12;5:34.

42. Hip resurfacing-OrthoInfo [Internet]. American Academy of Orthopaedic Surgeons. 2014 [cited 2017 Oct 29]. Available from: http://orthoinfo.aaos.org/topic.cfm?topic=a00586

43. Knee replacement implants-OrthoInfo [Internet]. American Academy of Orthopaedic Surgeons. 2016 [cited 2017 Oct 29]. Available from: http://orthoinfo.aaos.org/topic.cfm?topic=a00221

44. Matassi F, Carulli C, Civinini R, Innocenti M. Cemented versus cementless fixation in total knee arthroplasty. Joints. 2014 Jan 8;1(3):121–5.

45. Abdulkarim A, Ellanti P, Motterlini N, Fahey T, O'Byrne JM. Cemented versus uncemented fixation in total hip replacement: a systematic review and meta-analysis of randomized controlled trials. Orthop Rev [Internet]. 2013 Mar 15 [cited 2017 Oct 29];5(1). Available from: https://www.ncbi.nlm.nih.gov/pmc/articles/PMC3662257/

46. Howard JL, Kremers HM, Loechler YA, Schleck CD, Harmsen WS, Berry DJ, et al. Comparative survival of uncemented acetabular components following primary total hip arthroplasty. J Bone Joint Surg Am. 2011 Sep 7;93(17):1597–604.

47. Katti KS. Biomaterials in total joint replacement. Colloids Surf B Biointerfaces. 2004 Dec 10;39(3):133–42.

48. Affatato S, Ruggiero A, Merola M. Advanced biomaterials in hip joint arthroplasty. A review on polymer and ceramics composites as alternative bearings. Compos Part B Eng. 2015 Dec 15;83(Supplement C):276–83.

49. Kumar N, Arora GNC, Datta B. Bearing surfaces in hip replacement – Evolution and likely future. Med J Armed Forces India. 2014 Oct;70(4):371–6.

50. Pajarinen J, Jamsen E, Konttinen YT, Goodman SB. Innate immune reactions in septic and aseptic osteolysis around hip implants. J Long Term Eff Med Implants. 2014;24(4):283–96.

51. Gallo J, Goodman SB, Konttinen YT, Raska M. Particle disease: biologic mechanisms of periprosthetic osteolysis in total hip arthroplasty. Innate Immun. 2013 Apr 1;19(2):213–24.

52. Greenfield EM, Bechtold J, Implant Wear Symposium 2007 Biologic Work Group. What other biologic and mechanical factors might contribute to osteolysis? J Am Acad Orthop Surg. 2008;16 Suppl 1:S56-62.

53. Zimmerli W, Trampuz A, Ochsner PE. Prosthetic-joint infections. N Engl J Med. 2004 Oct 14;351(16):1645–54.

54. Lewallen DG. Historical aspects of bearing surfaces in total joint arthroplasty. American Association of Orthopaedic Surgeons 2015 Annual Meeting; 2015 Mar 27; Las Vegas, NV.

55. Knight SR, Aujla R, Biswas SP. Total hip arthroplasty - over 100 years of operative history. Orthop Rev. 2011 Sep 6;3(2):e16.

56. Kurtz SM. 1st and 2nd generation HXLPE: lessons from retrieval analysis. American Association of Orthopaedic Surgeons 2015 Annual Meeting; 2015 Mar 27; Las Vegas, NV.

57. Greenwald AS. Alternative Bearing Surfaces: An Evolution in Time. American Association of Orthopaedic Surgeons 2015 Annual Meeting; 2015 Mar 27; Las Vegas, NV.

58. Sakellariou VI, Sculco P, Poultsides L, Wright T, Sculco TP. Highly cross-linked polyethylene may not have an advantage in total knee arthroplasty. HSS J. 2013 Oct;9(3):264–9.

59. Bracco P, Bellare A, Bistolfi A, Affatato S. Ultra-high molecular weight polyethylene: influence of the chemical, physical and mechanical properties on the wear behavior. A review. Materials [Internet]. 2017 Jul 13 [cited 2017 Oct 30];10(7). Available from: https://www.ncbi.nlm.nih.gov/pmc/articles/PMC5551834/

60. de Guia N. Choice of bearing surface for total hip replacement affects need for repeat surgery: A Canadian perspective. 2014 Canadian Association of Health Services and Policy Research (CAHSPR) Conference; 2014 May; Toronto, ON.

61. Jiranek WA. What are the clinical results of cross-linked poly articulations? Cross Linked Poly in the Hip: Registries and Metanalysis. American Association of Orthopaedic Surgeons 2015 Annual Meeting; 2015 Mar 27; Las Vegas, NV.

62. Wright TM. Ceramic-on-ceramic perspective from a material scientist. American Association of Orthopaedic Surgeons 2015 Annual Meeting; 2015 Mar 27; Las Vegas, NV.

63. Bal BS, Garino J, Ries M, Rahaman MN. A review of ceramic bearing materials in total joint arthroplasty. Hip Int J Clin Exp Res Hip Pathol Ther. 2007 Mar;17(1):21–30.

64. Boutin P. [Total arthroplasty of the hip by fritted aluminum prosthesis. Experimental study and 1st clinical applications]. Rev Chir Orthop Reparatrice Appar Mot. 1972 May;58(3):229–46.

65. Wang T, Sun J-Y, Zhao X-J, Liu Y, Yin H. Ceramic-on-ceramic bearings total hip arthroplasty in young patients. Arthroplasty Today. 2016 Dec 1;2(4):205–9.

66. Lee Y-K, Yoon B-H, Choi YS, Jo W-L, Ha Y-C, Koo K-H. Metal on metal or ceramic on ceramic for cementless total hip arthroplasty: A meta-analysis. J Arthroplasty. 2016 Nov;31(11):2637–2645.e1.

67. Barrack RL. Ceramic-on-ceramic: clinician viewpoints. American Association of Orthopaedic Surgeons 2015 Annual Meeting; 2015 Mar 27; Las Vegas, NV.

68. Wu G-L, Zhu W, Zhao Y, Ma Q, Weng X-S. Hip squeaking after ceramic-on-ceramic total hip arthroplasty. Chin Med J (Engl). 2016 Aug 5;129(15):1861–6.

69. de Villiers D, Traynor A, Collins SN, Shelton JC. The increase in cobalt release in metal-on-polyethylene hip bearings in tests with third body abrasives. Proc Inst Mech Eng [H]. 2015 Sep;229(9):611–8.

70. Liao Y, Hoffman E, Wimmer M, Fischer A, Jacobs J, Marks L. CoCrMo metal-on-metal hip replacements. Phys Chem Chem Phys PCCP [Internet]. 2013 Jan 21 [cited 2017 Oct 30];15(3). Available from: https://www.ncbi.nlm.nih.gov/pmc/articles/PMC3530782/

71. Xia Z, Ricciardi BF, Liu Z, von Ruhland C, Ward M, Lord A, et al. Nano-analyses of wear particles from metal-on-metal and non-metal-on-metal dual modular neck hip arthroplasty. Nanomedicine Nanotechnol Biol Med. 2017 Apr 1;13(3):1205–17.

72. Doorn PF, Campbell PA, Worrall J, Benya PD, McKellop HA, Amstutz HC. Metal wear particle characterization from metal on metal total hip replacements: transmission electron microscopy study of periprosthetic tissues and isolated particles. J Biomed Mater Res. 1998 Oct;42(1):103–11.

73. Catelas I, Campbell PA, Bobyn JD, Medley JB, Huk OL. Wear particles from metal-on-metal total hip replacements: effects of implant design and implantation time. Proc Inst Mech Eng [H]. 2006 Feb;220(2):195–208.

74. Kobayashi A, Bonfield W, Kadoya Y, Yamac T, Freeman MA, Scott G, et al. The size and shape of particulate polyethylene wear debris in total joint replacements. Proc Inst Mech Eng [H]. 1997 Jan;211(1):11–5.

75. Campbell P, Ma S, Yeom B, McKellop H, Schmalzried TP, Amstutz HC. Isolation of predominantly submicron-sized UHMWPE wear particles from periprosthetic tissues. J Biomed Mater Res. 1995 Jan;29(1):127–31.

76. Visentin M, Stea S, Squarzoni S, Antonietti B, Reggiani M, Toni A. A new method for isolation of polyethylene wear debris from tissue and synovial fluid. Biomaterials. 2004 Nov;25(24):5531–7.

77. Nakano N, Volpin A, Bartlett J, Khanduja V. Management guidelines for metal-on-metal hip resurfacing arthroplasty: A strategy on followup. Indian J Orthop. 2017 Jul;51(4):414–20.

78. Berber R, Skinner JA, Hart AJ. Management of metal-on-metal hip implant patients: Who, when and how to revise? World J Orthop. 2016 May 18;7(5):272–9.

79. ASR Recall [Internet]. DePuy Synthes. 2015 [cited 2017 Nov 27]. Available from: https://www.depuysynthes.com/asrrecall/asrcanadaenglish.html

80. Health C for D and R. Metal-on-metal hip implants - Concerns about metal-on-metal hip implants [Internet]. U.S. Food and Drug Administration. 2017 [cited 2017 Nov 27]. Available from: https://www.fda.gov/MedicalDevices/ProductsandMedicalProcedures/ImplantsandProsthetics/MetalonMetalHipImplants/ucm241604.htm

81. Silva M, Heisel C, Schmalzried TP. Metal-on-metal total hip replacement. Clin Orthop. 2005 Jan;(430):53–61.

82. Silverman EJ, Ashley B, Sheth NP. Metal-on-metal total hip arthroplasty: is there still a role in 2016? Curr Rev Musculoskelet Med. 2016 Jan 20;9(1):93–6.

83. Pastides PS, Dodd M, Sarraf KM, Willis-Owen CA. Trunnionosis: A pain in the neck. World J Orthop. 2013 Oct 18;4(4):161–6.

84. Mistry JB, Chughtai M, Elmallah RK, Diedrich A, Le S, Thomas M, et al. Trunnionosis in total hip arthroplasty: a review. J Orthop Traumatol Off J Ital Soc Orthop Traumatol. 2016 Mar;17(1):1–6.

85. Charette RS, Neuwirth AL, Nelson CL. Arthroprosthetic cobaltism associated with cardiomyopathy. Arthroplasty Today [Internet]. 2016 Dec 15 [cited 2017 Nov 27]; Available from: http://www.sciencedirect.com/science/article/pii/S2352344116300723

86. Willert HG, Semlitsch M. Reactions of the articular capsule to wear products of artificial joint prostheses. J Biomed Mater Res. 1977 Mar;11(2):157–64.

87. Jones LC, Hungerford DS. Cement disease. Clin Orthop. 1987 Dec;(225):192–206.

88. Harris WH. Osteolysis and particle disease in hip replacement. A review. Acta Orthop Scand. 1994 Feb;65(1):113–23.

89. Purdue PE, Koulouvaris P, Nestor BJ, Sculco TP. The central role of wear debris in periprosthetic osteolysis. HSS J. 2006 Sep 1;2(2):102–13.

90. Konttinen YT, Pajarinen J, Takakubo Y, Gallo J, Nich C, Takagi M, et al. Macrophage polarization and activation in response to implant debris: influence by “particle disease” and “ion disease.” J Long Term Eff Med Implants. 2014;24(4):267–81.

91. Nich C, Takakubo Y, Pajarinen J, Ainola M, Salem A, Sillat T, et al. Macrophages—Key cells in the response to wear debris from joint replacements. J Biomed Mater Res A. 2013 Oct 1;101(10):3033–45.

92. Ginhoux F, Jung S. Monocytes and macrophages: developmental pathways and tissue homeostasis. Nat Rev Immunol. 2014 Jun;14(6):392–404.

93. Cobelli N, Scharf B, Crisi GM, Hardin J, Santambrogio L. Mediators of the inflammatory response to joint replacement devices. Nat Rev Rheumatol. 2011 Sep 6;7(10):600–8.

94. Catelas I, Petit A, Zukor DJ, Antoniou J, Huk OL. TNF-alpha secretion and macrophage mortality induced by cobalt and chromium ions in vitro-qualitative analysis of apoptosis. Biomaterials. 2003 Feb;24(3):383–91.

95. Blaine TA, Rosier RN, Puzas JE, Looney RJ, Reynolds PR, Reynolds SD, et al. Increased levels of tumor necrosis factor-alpha and interleukin-6 protein and messenger RNA in human peripheral blood monocytes due to titanium particles. J Bone Joint Surg Am. 1996 Aug;78(8):1181–92.

96. Bukata SV, Gelinas J, Wei X, Rosier RN, Puzas JE, Zhang X, et al. PGE2 and IL-6 production by fibroblasts in response to titanium wear debris particles is mediated through a Cox-2 dependent pathway. J Orthop Res Off Publ Orthop Res Soc. 2004 Jan;22(1):6–12.

97. Baskey SJ, Beaulé PE, Lehoux EA, Catelas I. Simvastatin modulates the release of TNF-α and CC chemokines from macrophages exposed to trivalent chromium ions. J Biomater Tissue Eng. 2014 Nov 1;4(11):981–91.

98. Clarke SA, Brooks RA, Hobby JL, Wimhurst JA, Myer BJ, Rushton N. Correlation of synovial fluid cytokine levels with histological and clinical parameters of primary and revision total hip and total knee replacements. Acta Orthop Scand. 2001 Oct;72(5):491–8.

99. Davies AP, Willert HG, Campbell PA, Learmonth ID, Case CP. An unusual lymphocytic perivascular infiltration in tissues around contemporary metal-on-metal joint replacements. J Bone Joint Surg Am. 2005 Jan;87(1):18–27.

100. Haynes DR, Crotti TN, Potter AE, Loric M, Atkins GJ, Howie DW, et al. The osteoclastogenic molecules RANKL and RANK are associated with periprosthetic osteolysis. J Bone Joint Surg Br. 2001 Aug;83(6):902–11.

101. Wang C-T, Lin Y-T, Chiang B-L, Lee S-S, Hou S-M. Over-expression of receptor activator of nuclear factor-kappaB ligand (RANKL), inflammatory cytokines, and chemokines in periprosthetic osteolysis of loosened total hip arthroplasty. Biomaterials. 2010 Jan;31(1):77–82.

102. Zijlstra WP, Bulstra SK, van Raay JJAM, van Leeuwen BM, Kuijer R. Cobalt and chromium ions reduce human osteoblast-like cell activity in vitro, reduce the OPG to RANKL ratio, and induce oxidative stress. J Orthop Res Off Publ Orthop Res Soc. 2012 May;30(5):740–7.

103. Wang ML, Nesti LJ, Tuli R, Lazatin J, Danielson KG, Sharkey PF, et al. Titanium particles suppress expression of osteoblastic phenotype in human mesenchymal stem cells. J Orthop Res Off Publ Orthop Res Soc. 2002 Nov;20(6):1175–84.

104. Vermes C, Chandrasekaran R, Jacobs JJ, Galante JO, Roebuck KA, Glant TT. The effects of particulate wear debris, cytokines, and growth factors on the functions of MG-63 osteoblasts. J Bone Joint Surg Am. 2001 Feb;83–A(2):201–11.

105. Fukata M, Vamadevan AS, Abreu MT. Toll-like receptors (TLRs) and Nod-like receptors (NLRs) in inflammatory disorders. Semin Immunol. 2009 Aug;21(4):242–53.

106. Kawai T, Akira S. The roles of TLRs, RLRs and NLRs in pathogen recognition. Int Immunol. 2009 Apr;21(4):317–37.

107. Bauernfeind FG, Horvath G, Stutz A, Alnemri ES, MacDonald K, Speert D, et al. Cutting edge: NF-κB activating pattern recognition and cytokine receptors license NLRP3 inflammasome activation by regulating NLRP3 expression. J Immunol. 2009 Jul 15;183(2):787–91.

108. Hoesel B, Schmid JA. The complexity of NF-κB signaling in inflammation and cancer. Mol Cancer. 2013 Aug 2;12:86.

109. Maitra R, Clement CC, Crisi GM, Cobelli N, Santambrogio L. Immunogenecity of modified alkane polymers is mediated through TLR1/2 activation. PLoS ONE. 2008 Jun 18;3(6):e2438.

110. Tyson-Capper AJ, Lawrence H, Holland JP, Deehan DJ, Kirby JA. Metal-on-metal hips: cobalt can induce an endotoxin-like response. Ann Rheum Dis. 2013 Mar;72(3):460–1.

111. Nelson CL, McLaren AC, McLaren SG, Johnson JW, Smeltzer MS. Is aseptic loosening truly aseptic? Clin Orthop. 2005 Aug;(437):25–30.

112. Caicedo MS, Samelko L, McAllister K, Jacobs JJ, Hallab NJ. Increasing both CoCrMo-alloy particle size and surface irregularity induces increased macrophage inflammasome activation in vitro potentially through lysosomal destabilization mechanisms. J Orthop Res. 2013 Oct 1;31(10):1633–42.

113. Samelko L, Landgraeber S, McAllister K, Jacobs J, Hallab NJ. Cobalt alloy implant debris induces inflammation and bone loss primarily through danger signaling, not TLR4 activation: implications for DAMP-ening implant related inflammation. PLoS ONE. 2016 Jul 28;11(7):e0160141.

114. Sutterwala FS, Haasken S, Cassel SL. Mechanism of NLRP3 inflammasome activation. Ann N Y Acad Sci. 2014 Jun;1319(1):82–95.

115. Campbell P, Ebramzadeh E, Nelson S, Takamura K, De Smet K, Amstutz HC. Histological features of pseudotumor-like tissues from metal-on-metal hips. Clin Orthop. 2010 Sep;468(9):2321–7.

116. Wang Y, Dai S. Structural basis of metal hypersensitivity. Immunol Res. 2013 Mar;55(1–3):83–90.

117. Bitar D, Parvizi J. Biological response to prosthetic debris. World J Orthop. 2015 Mar 18;6(2):172–89.

118. Kandahari AM, Yang X, Laroche KA, Dighe AS, Pan D, Cui Q. A review of UHMWPE wear-induced osteolysis: the role for early detection of the immune response. Bone Res. 2016 Jul;4:16014.

119. Milosev I, Trebse R, Kovac S, Cör A, Pisot V. Survivorship and retrieval analysis of Sikomet metal-on-metal total hip replacements at a mean of seven years. J Bone Joint Surg Am. 2006 Jun;88(6):1173–82.

120. Jacobs JJ, Hallab NJ. Loosening and osteolysis associated with metal-on-metal bearings: A local effect of metal hypersensitivity? J Bone Joint Surg Am. 2006 Jun;88(6):1171–2.

121. Metal-on-metal hip implants – Information for orthopaedic surgeons regarding patient management following surgery – For the public [Internet]. Government of Canada. 2012 [cited 2017 Oct 30]. Available from: http://www.healthycanadians.gc.ca/recall-alert-rappel-avis/hc-sc/2012/14120a-eng.php

122. Mabilleau G, Kwon Y-M, Pandit H, Murray DW, Sabokbar A. Metal-on-metal hip resurfacing arthroplasty: a review of periprosthetic biological reactions. Acta Orthop. 2008 Dec;79(6):734–47.

123. Martinon F, Burns K, Tschopp J. The inflammasome: a molecular platform triggering activation of inflammatory caspases and processing of proIL-beta. Mol Cell. 2002 Aug;10(2):417–26.

124. Adam C, Wohlfarth J, Haußmann M, Sennefelder H, Rodin A, Maler M, et al. Allergy-inducing chromium compounds trigger potent innate immune stimulation via ROS-dependent inflammasome activation. J Invest Dermatol. 2017 Feb 1;137(2):367–76.

125. Martinon F, Mayor A, Tschopp J. The inflammasomes: guardians of the body. Annu Rev Immunol. 2009 Apr;27:229–65.

126. Kostura MJ, Tocci MJ, Limjuco G, Chin J, Cameron P, Hillman AG, et al. Identification of a monocyte specific pre-interleukin 1 beta convertase activity. Proc Natl Acad Sci U S A. 1989 Jul;86(14):5227–31.

127. Black RA, Kronheim SR, Sleath PR. Activation of interleukin-1 beta by a co-induced protease. FEBS Lett. 1989 Apr 24;247(2):386–90.

128. Thornberry NA, Molineaux SM. Interleukin-1 beta converting enzyme: a novel cysteine protease required for IL-1 beta production and implicated in programmed cell death. Protein Sci Publ Protein Soc. 1995 Jan;4(1):3–12.

129. Tocci MJ. Structure and function of interleukin-1 beta converting enzyme. Vitam Horm. 1997;53:27–63.

130. Thornberry NA, Bull HG, Calaycay JR, Chapman KT, Howard AD, Kostura MJ, et al. A novel heterodimeric cysteine protease is required for interleukin-1 beta processing in monocytes. Nature. 1992 Apr 30;356(6372):768–74.

131. Hoffman HM, Mueller JL, Broide DH, Wanderer AA, Kolodner RD. Mutation of a new gene encoding a putative pyrin-like protein causes familial cold autoinflammatory syndrome and Muckle-Wells syndrome. Nat Genet. 2001 Nov;29(3):301–5.

132. Feldmann J, Prieur A-M, Quartier P, Berquin P, Certain S, Cortis E, et al. Chronic infantile neurological cutaneous and articular syndrome is caused by mutations in CIAS1, a gene highly expressed in polymorphonuclear cells and chondrocytes. Am J Hum Genet. 2002 Jul;71(1):198–203.

133. Aksentijevich I, Nowak M, Mallah M, Chae JJ, Watford WT, Hofmann SR, et al. De novo CIAS1 mutations, cytokine activation, and evidence for genetic heterogeneity in patients with neonatal-onset multisystem inflammatory disease (NOMID): a new member of the expanding family of pyrin-associated autoinflammatory diseases. Arthritis Rheum. 2002 Dec;46(12):3340–8.

134. Chavarría-Smith J, Vance RE. Direct proteolytic cleavage of NLRP1B is necessary and sufficient for inflammasome activation by anthrax lethal factor. PLoS Pathog. 2013 Jun;9(6):e1003452.

135. Chavarría-Smith J, Vance RE. The NLRP1 inflammasomes. Immunol Rev. 2015 May;265(1):22–34.

136. Zhao Y, Shao F. The NAIP-NLRC4 inflammasome in innate immune detection of bacterial flagellin and type III secretion apparatus. Immunol Rev. 2015 May;265(1):85–102.

137. Vance RE. The NAIP/NLRC4 inflammasomes. Curr Opin Immunol. 2015 Feb;0:84–9.

138. Rathinam VAK, Jiang Z, Waggoner SN, Sharma S, Cole LE, Waggoner L, et al. The AIM2 inflammasome is essential for host defense against cytosolic bacteria and DNA viruses. Nat Immunol. 2010 May;11(5):395–402.

139. He Y, Hara H, Núñez G. Mechanism and regulation of NLRP3 inflammasome activation. Trends Biochem Sci. 2016 Dec;41(12):1012–21.

140. Dostert C, Guarda G, Romero JF, Menu P, Gross O, Tardivel A, et al. Malarial hemozoin is a NALP3 inflammasome activating danger signal. PLoS ONE. 2009 Aug 4;4(8):e6510.

141. Martinon F, Pétrilli V, Mayor A, Tardivel A, Tschopp J. Gout-associated uric acid crystals activate the NALP3 inflammasome. Nature. 2006 Mar 9;440(7081):237–41.

142. Dostert C, Pétrilli V, Bruggen RV, Steele C, Mossman BT, Tschopp J. Innate immune activation through NALP3 inflammasome sensing of asbestos and silica. Science. 2008 May 2;320(5876):674–7.

143. Samelko L, Caicedo MS, Lim S-J, Della-Valle C, Jacobs J, Hallab NJ. Cobalt-alloy implant debris induce HIF-1α hypoxia associated responses: a mechanism for metal-specific orthopedic implant failure. PLoS ONE. 2013 Jun 20;8(6):e67127.

144. Hornung V, Bauernfeind F, Halle A, Samstad EO, Kono H, Rock KL, et al. Silica crystals and aluminum salts activate the NALP3 inflammasome through phagosomal destabilization. Nat Immunol. 2008 Aug;9(8):847–56.

145. Latz E, Xiao TS, Stutz A. Activation and regulation of the inflammasomes. Nat Rev Immunol [Internet]. 2013 Jun [cited 2017 Aug 15];13(6). Available from: http://www.ncbi.nlm.nih.gov/pmc/articles/PMC3807999/

146. Patel MN, Carroll RG, Galván-Peña S, Mills EL, Olden R, Triantafilou M, et al. Inflammasome priming in sterile inflammatory disease. Trends Mol Med. 2017 Feb 1;23(2):165–80.

147. Shamaa OR, Mitra S, Gavrilin MA, Wewers MD. Monocyte caspase-1 is released in a stable, active high molecular weight complex distinct from the unstable cell lysate-activated caspase-1. PLoS ONE. 2015 Nov 24;10(11):e0142203.

148. Baroja-Mazo A, Martín-Sánchez F, Gomez AI, Martínez CM, Amores-Iniesta J, Compan V, et al. The NLRP3 inflammasome is released as a particulate danger signal that amplifies the inflammatory response. Nat Immunol. 2014 Aug;15(8):738–48.

149. Elliott EI, Sutterwala FS. Initiation and perpetuation of NLRP3 inflammasome activation and assembly. Immunol Rev. 2015 May;265(1):35–52.

150. Franchi L, Eigenbrod T, Núñez G. Cutting edge: TNF-alpha mediates sensitization to ATP and silica via the NLRP3 inflammasome in the absence of microbial stimulation. J Immunol Baltim Md 1950. 2009 Jul 15;183(2):792–6.

151. Gurung P, Li B, Subbarao Malireddi RK, Lamkanfi M, Geiger TL, Kanneganti T-D. Chronic TLR stimulation controls NLRP3 inflammasome activation through IL-10 mediated regulation of NLRP3 expression and caspase-8 activation. Sci Rep [Internet]. 2015 Sep 28 [cited 2017 Aug 19]. Available from: http://www.ncbi.nlm.nih.gov/pmc/articles/PMC4585974/

152. Ghonime MG, Shamaa OR, Das S, Eldomany RA, Fernandes-Alnemri T, Alnemri ES, et al. Inflammasome priming by lipopolysaccharide is dependent upon ERK signaling and proteasome function. J Immunol. 2014 Apr 15;192(8):3881–8.

153. Afonina IS, Zhong Z, Karin M, Beyaert R. Limiting inflammation—the negative regulation of NF-κB and the NLRP3 inflammasome. Nat Immunol. 2017 Aug;18(8):861–9.

154. Juliana C, Fernandes-Alnemri T, Kang S, Farias A, Qin F, Alnemri ES. Non-transcriptional priming and deubiquitination regulate NLRP3 inflammasome activation. J Biol Chem. 2012 Oct 19;287(43):36617–22.

155. Bi Y, Seabold JM, Kaar SG, Ragab AA, Goldberg VM, Anderson JM, et al. Adherent endotoxin on orthopedic wear particles stimulates cytokine production and osteoclast differentiation. J Bone Miner Res Off J Am Soc Bone Miner Res. 2001 Nov;16(11):2082–91.

156. Bi Y, Collier TO, Goldberg VM, Anderson JM, Greenfield EM. Adherent endotoxin mediates biological responses of titanium particles without stimulating their phagocytosis. J Orthop Res Off Publ Orthop Res Soc. 2002 Jul;20(4):696–703.

157. Greenfield EM, Bi Y, Ragab AA, Goldberg VM, Nalepka JL, Seabold JM. Does endotoxin contribute to aseptic loosening of orthopedic implants? J Biomed Mater Res B Appl Biomater. 2005 Jan 15;72(1):179–85.

158. Greenfield EM, Beidelschies MA, Tatro JM, Goldberg VM, Hise AG. Bacterial pathogen-associated molecular patterns stimulate biological activity of orthopaedic wear particles by activating cognate Toll-like receptors. J Biol Chem. 2010 Oct 15;285(42):32378–84.

159. Manzano G, Fort B, Dubyak GR, Greenfield EM. Priming of the NLRP3 inflammasome by orthopaedic wear particles depends on adherent PAMPs and their cognate Toll-like receptors. In: Orthopaedic Research Society 2017 Annual Meeting. 2017.

160. Samelko L, Landgraeber S, McAllister K, Jacobs J, Hallab NJ. TLR4 (not TLR2) dominate cognate TLR activity associated with CoCrMo implant particles. J Orthop Res. 2017 May 1;35(5):1007–17.

161. Pétrilli V, Papin S, Dostert C, Mayor A, Martinon F, Tschopp J. Activation of the NALP3 inflammasome is triggered by low intracellular potassium concentration. Cell Death Differ. 2007 Jun 29;14(9):1583–9.

162. Segovia J, Sabbah A, Mgbemena V, Tsai S-Y, Chang T-H, Berton MT, et al. TLR2/MyD88/NF-κB pathway, reactive oxygen species, potassium efflux activates NLRP3/ASC inflammasome during respiratory syncytial virus infection. PLoS ONE. 2012 Jan;7(1):e29695.

163. Muñoz-Planillo R, Kuffa P, Martínez-Colón G, Smith BL, Rajendiran TM, Núñez G. K+ efflux Is the common trigger of NLRP3 inflammasome activation by bacterial toxins and particulate matter. Immunity. 2013 Jun 27;38(6):1142–53.

164. Perregaux D, Gabel CA. Interleukin-1 beta maturation and release in response to ATP and nigericin. Evidence that potassium depletion mediated by these agents is a necessary and common feature of their activity. J Biol Chem. 1994 May 27;269(21):15195–203.

165. Alonso MA, Carrasco L. Permeabilization of mammalian cells to proteins by the ionophore nigericin. FEBS Lett. 1981 May 5;127(1):112–4.

166. Gombault A, Baron L, Couillin I. ATP release and purinergic signaling in NLRP3 inflammasome activation. Front Immunol [Internet]. 2013 Jan 8 [cited 2017 Oct 17];3. Available from: https://www.ncbi.nlm.nih.gov/pmc/articles/PMC3539150/

167. Franceschini A, Capece M, Chiozzi P, Falzoni S, Sanz JM, Sarti AC, et al. The P2X7 receptor directly interacts with the NLRP3 inflammasome scaffold protein. FASEB J Off Publ Fed Am Soc Exp Biol. 2015 Jun;29(6):2450–61.

168. Rossol M, Pierer M, Raulien N, Quandt D, Meusch U, Rothe K, et al. Extracellular Ca^{2+} is a danger signal activating the NLRP3 inflammasome through G protein-coupled calcium sensing receptors. Nat Commun. 2012 Dec;3:1329.

169. Lee G-S, Subramanian N, Kim AI, Aksentijevich I, Goldbach-Mansky R, Sacks DB, et al. The calcium-sensing receptor regulates the NLRP3 inflammasome through Ca^{2+} and cAMP. Nature. 2012 Dec 6;492(7427):123–7.

170. Murakami T, Ockinger J, Yu J, Byles V, McColl A, Hofer AM, et al. Critical role for calcium mobilization in activation of the NLRP3 inflammasome. Proc Natl Acad Sci U S A. 2012 Jul 10;109(28):11282–7.

171. Triantafilou K, Hughes TR, Triantafilou M, Morgan BP. The complement membrane attack complex triggers intracellular Ca^{2+} fluxes leading to NLRP3 inflammasome activation. J Cell Sci. 2013 Jul 1;126(Pt 13):2903–13.

172. Li X, Zhong F. Nickel induces interleukin-1β secretion via the NLRP3-ASC-caspase-1 pathway. Inflammation. 2014 Apr;37(2):457–66.

173. Zhong Z, Zhai Y, Liang S, Mori Y, Han R, Sutterwala FS, et al. TRPM2 links oxidative stress to NLRP3 inflammasome activation. Nat Commun. 2013 Mar;4:1611.

174. Gross O, Yazdi AS, Thomas CJ, Masin M, Heinz LX, Guarda G, et al. Inflammasome activators induce interleukin-1α secretion via distinct pathways with differential requirement for the protease function of caspase-1. Immunity. 2012 Mar 23;36(3):388–400.

175. Yaron JR, Gangaraju S, Rao MY, Kong X, Zhang L, Su F, et al. K(+) regulates Ca(2+) to drive inflammasome signaling: dynamic visualization of ion flux in live cells. Cell Death Dis. 2015 Oct 29;6:e1954.

176. Meunier E, Coste A, Olagnier D, Authier H, Lefèvre L, Dardenne C, et al. Double-walled carbon nanotubes trigger IL-1β release in human monocytes through Nlrp3 inflammasome activation. Nanomedicine Nanotechnol Biol Med. 2012 Aug 1;8(6):987–95.

177. Halle A, Hornung V, Petzold GC, Stewart CR, Monks BG, Reinheckel T, et al. The NALP3 inflammasome is involved in the innate immune response to amyloid-β. Nat Immunol. 2008 Aug;9(8):857–65.

178. Maitra R, Clement CC, Scharf B, Crisi GM, Chitta S, Paget D, et al. Endosomal damage and TLR2 mediated inflammasome activation by alkane particles in the generation of aseptic osteolysis. Mol Immunol. 2009 Dec;47(2–3):175–84.

179. Jin C, Flavell RA. Molecular mechanism of NLRP3 inflammasome activation. J Clin Immunol. 2010 Sep 1;30(5):628–31.

180. Orlowski GM, Colbert JD, Sharma S, Bogyo M, Robertson SA, Rock KL. Multiple cathepsins promote pro-IL-1β synthesis and NLRP3-mediated IL-1β activation. J Immunol Baltim Md 1950. 2015 Aug 15;195(4):1685–97.

181. Hornung V, Latz E. Critical functions of priming and lysosomal damage for NLRP3 activation. Eur J Immunol. 2010 Mar;40(3):620–3.

182. Zhou R, Yazdi AS, Menu P, Tschopp J. A role for mitochondria in NLRP3 inflammasome activation. Nature. 2011 Jan 13;469(7329):221–5.

183. Nakahira K, Haspel JA, Rathinam VAK, Lee S-J, Dolinay T, Lam HC, et al. Autophagy proteins regulate innate immune responses by inhibiting the release of mitochondrial DNA mediated by the NALP3 inflammasome. Nat Immunol. 2011 Mar;12(3):222–30.

184. Shimada K, Crother TR, Karlin J, Dagvadorj J, Chiba N, Chen S, et al. Oxidized mitochondrial DNA activates the NLRP3 inflammasome during apoptosis. Immunity. 2012 Mar 23;36(3):401–14.

185. Misawa T, Takahama M, Kozaki T, Lee H, Zou J, Saitoh T, et al. Microtubule-driven spatial arrangement of mitochondria promotes activation of the NLRP3 inflammasome. Nat Immunol. 2013 May;14(5):454–60.

186. Iyer SS, He Q, Janczy JR, Elliott EI, Zhong Z, Olivier AK, et al. Mitochondrial cardiolipin is required for Nlrp3 inflammasome activation. Immunity. 2013 Aug 22;39(2):311–23.

187. Ichinohe T, Yamazaki T, Koshiba T, Yanagi Y. Mitochondrial protein mitofusin 2 is required for NLRP3 inflammasome activation after RNA virus infection. Proc Natl Acad Sci U S A. 2013 Oct 29;110(44):17963–8.

188. Sang X, Wang H, Chen Y, Guo Q, Lu A, Zhu X, et al. Vitamin C inhibits the activation of the NLRP3 inflammasome by scavenging mitochondrial ROS. Inflammasome. 2016 Mar;2(1):13–19.

189. Drummond GR, Selemidis S, Griendling KK, Sobey CG. Combating oxidative stress in vascular disease: NADPH oxidases as therapeutic targets. Nat Rev Drug Discov. 2011 Jun;10(6):453–71.

190. van Bruggen R, Köker MY, Jansen M, van Houdt M, Roos D, Kuijpers TW, et al. Human NLRP3 inflammasome activation is Nox1-4 independent. Blood. 2010 Jul 1;115(26):5398–400.

191. Stohs SJ, Bagchi D. Oxidative mechanisms in the toxicity of metal ions. Free Radic Biol Med. 1995 Feb;18(2):321–36.

192. Catelas I, Petit A, Zukor DJ, Huk OL. Cytotoxic and apoptotic effects of cobalt and chromium ions on J774 macrophages – Implication of caspase-3 in the apoptotic pathway. J Mater Sci Mater Med. 2001 Dec 1;12(10–12):949–53.

193. Catelas I, Petit A, Vali H, Fragiskatos C, Meilleur R, Zukor DJ, et al. Quantitative analysis of macrophage apoptosis vs. necrosis induced by cobalt and chromium ions in vitro. Biomaterials. 2005 May;26(15):2441–53.

194. Baskey SJ, Lehoux EA, Catelas I. Effects of cobalt and chromium ions on lymphocyte migration. J Orthop Res. 2017 Apr 1;35(4):916–24.

195. Mantripragada VP, Lecka-Czernik B, Ebraheim NA, Jayasuriya AC. An overview of recent advances in designing orthopedic and craniofacial implants. J Biomed Mater Res A. 2013 Nov;101(11):3349–64.

196. Jacobs JJ, Gilbert JL, Urban RM. Corrosion of metal orthopaedic implants. J Bone Joint Surg Am. 1998 Feb;80(2):268–82.

197. Goodman SB, Gómez Barrena E, Takagi M, Konttinen YT. Biocompatibility of total joint replacements: A review. J Biomed Mater Res A. 2009 Aug;90(2):603–18.

198. Skipor AK, Campbell PA, Patterson LM, Anstutz HC, Schmalzried TP, Jacobs JJ. Serum and urine metal levels in patients with metal-on-metal surface arthroplasty. J Mater Sci Mater Med. 2002 Dec;13(12):1227–34.

199. Rasquinha VJ, Ranawat CS, Weiskopf J, Rodriguez JA, Skipor AK, Jacobs JJ. Serum metal levels and bearing surfaces in total hip arthroplasty. J Arthroplasty. 2006 Sep 1;21(6):47–52.

200. Hartmann A, Hannemann F, Lützner J, Seidler A, Drexler H, Günther K-P, et al. Metal ion concentrations in body fluids after implantation of hip replacements with metal-on-metal bearing--systematic review of clinical and epidemiological studies. PLoS ONE. 2013 Aug;8(8):e70359.

201. Bauer TW, Campbell PA, Hallerberg G. How have new bearing surfaces altered the local biological reactions to byproducts of wear and modularity? Clin Orthop. 2014 Dec;472(12):3687–98.

202. Kwon Y-M, Fehring TK, Lombardi AV, Barnes CL, Cabanela ME, Jacobs JJ. Risk stratification algorithm for management of patients with dual modular taper total hip arthroplasty: consensus statement of the american association of hip and knee surgeons, the american cademy of orthopaedic surgeons and the hip society. J Arthroplasty. 2014 Nov 1;29(11):2060–4.

203. Willert H-G, Buchhorn GH, Fayyazi A, Flury R, Windler M, Köster G, et al. Metal-on-metal bearings and hypersensitivity in patients with artificial hip joints. A clinical and histomorphological study. J Bone Joint Surg Am. 2005 Jan;87(1):28–36.

204. Kwon Y-M, Ostlere SJ, McLardy-Smith P, Athanasou NA, Gill HS, Murray DW. "Asymptomatic" pseudotumors after metal-on-metal hip resurfacing arthroplasty. J Arthroplasty. 2011 Jun 1;26(4):511–8.

205. Nich C, Goodman SB. Role of macrophages in the biological reaction to wear debris from joint replacements. J Long Term Eff Med Implants. 2014;24(4):259–65.

206. Ingham E, Fisher J. The role of macrophages in osteolysis of total joint replacement. Biomaterials. 2005 Apr;26(11):1271–86.

207. Phillips EA, Klein GR, Cates HE, Kurtz SM, Steinbeck M. Histological characterization of periprosthetic tissue responses for metal-on-metal hip replacement. J Long Term Eff Med Implants. 2014;24(1):13–23.

208. Verschoor CP, Puchta A, Bowdish DME. The macrophage. Methods Mol Biol Clifton NJ. 2011 Dec;844:139–56.

209. Gross O. Measuring the inflammasome. Methods Mol Biol Clifton NJ. 2011 Dec;844:199–222.

210. Davies JQ, Gordon S. Isolation and culture of murine macrophages. In: Basic Cell Culture Protocols [Internet]. Humana Press; 2005 [cited 2017 Sep 12]. p. 91–103. (Methods in Molecular Biology™). Available from: https://link.springer.com/protocol/10.1385/1-59259-838-2:091

211. Zhang X, Goncalves R, Mosser DM. The isolation and characterization of murine macrophages. Curr Protoc Immunol Ed John E Coligan Al. 2008 Nov;CHAPTER:Unit-14.1.

212. Marim FM, Silveira TN, Lima DS, Zamboni DS. A method for generation of bone marrow-derived macrophages from cryopreserved mouse bone marrow cells. PLoS ONE [Internet]. 2010 Dec 17 [cited 2018 Jan 4];5(12). Available from: https://www.ncbi.nlm.nih.gov/pmc/articles/PMC3003694/

213. Jakobs C, Bartok E, Kubarenko A, Bauernfeind F, Hornung V. Immunoblotting for active caspase-1. Methods Mol Biol Clifton NJ. 2013 Jun;1040:103–15.

214. Eisenbarth SC, Colegio OR, O'Connor W, Sutterwala FS, Flavell RA. Crucial role for the NALP3 inflammasome in the immunostimulatory properties of aluminium adjuvants. Nature. 2008 Jun 19;453(7198):1122–6.

215. Schroder K, Zhou R, Tschopp J. The NLRP3 inflammasome: a sensor for metabolic danger? Science. 2010 Jan 15;327(5963):296–300.

216. Tschopp J, Schroder K. NLRP3 inflammasome activation: The convergence of multiple signalling pathways on ROS production? Nat Rev Immunol. 2010 Mar;10(3):210–5.

217. Shin H-M, Kim M-H, Kim BH, Jung S-H, Kim YS, Park HJ, et al. Inhibitory action of novel aromatic diamine compound on lipopolysaccharide-induced nuclear translocation of NF-kappaB without affecting IkappaB degradation. FEBS Lett. 2004 Jul 30;571(1–3):50–4.

218. Kinoshita T, Imamura R, Kushiyama H, Suda T. NLRP3 mediates NF-κB activation and cytokine induction in microbially induced and sterile inflammation. PLoS ONE. 2015 Mar 11;10(3):e0119179.

219. Takagi M, Tamaki Y, Hasegawa H, Takakubo Y, Konttinen L, Tiainen V-M, et al. Toll-like receptors in the interface membrane around loosening total hip replacement implants. J Biomed Mater Res A. 2007 Jun 15;81(4):1017–26.

220. Lähdeoja T, Pajarinen J, Kouri V-P, Sillat T, Salo J, Konttinen YT. Toll-like receptors and aseptic loosening of hip endoprosthesis-a potential to respond against danger signals? J Orthop Res Off Publ Orthop Res Soc. 2010 Feb;28(2):184–90.

221. Takagi M, Takakubo Y, Pajarinen J, Naganuma Y, Oki H, Maruyama M, et al. Danger of frustrated sensors: Role of Toll-like receptors and NOD-like receptors in aseptic and septic inflammations around total hip replacements. J Orthop Transl. 2017 Jul 1;10:68–85.

222. Weischenfeldt J, Porse B. Bone marrow-derived macrophages (BMM): isolation and applications. CSH Protoc. 2008 Dec 1;2008:pdb.prot5080.

223. Lee CM, Hu J. Cell density during differentiation can alter the phenotype of bone marrow-derived macrophages. Cell Biosci. 2013 Jul 29;3:30.

224. Trouplin V, Boucherit N, Gorvel L, Conti F, Mottola G, Ghigo E. Bone marrow-derived macrophage production. J Vis Exp JoVE [Internet]. 2013 Nov 22 [cited 2017 Sep 12];(81). Available from: http://www.ncbi.nlm.nih.gov/pmc/articles/PMC3991821/

225. Fortier AH, Falk LA. Isolation of murine macrophages. In: Current Protocols in Immunology [Internet]. John Wiley & Sons, Inc.; 2001 [cited 2017 Nov 20]. Available from: http://onlinelibrary.wiley.com/doi/10.1002/0471142735.im1401s11/abstract

226. McComb S. The paradoxical roles of cell death pathways in immune cells [Internet] [PhD Thesis]. [Ottawa, ON]: University of Ottawa; 2013. Available from: https://ruor.uottawa.ca/bitstream/10393/24331/3/McComb_Scott_2013_thesis.pdf

227. Dos Anjos Cassado A. F4/80 as a major macrophage marker: The case of the peritoneum and spleen. Results Probl Cell Differ. 2017 Apr;62:161–79.

228. Lin H-H, Faunce DE, Stacey M, Terajewicz A, Nakamura T, Zhang-Hoover J, et al. The macrophage F4/80 receptor is required for the induction of antigen-specific efferent regulatory T cells in peripheral tolerance. J Exp Med. 2005 May 16;201(10):1615–25.

229. Lin H-H, Stacey M, Stein-Streilein J, Gordon S. F4/80: the macrophage-specific adhesion-GPCR and its role in immunoregulation. Adv Exp Med Biol. 2010 Jan;706:149–56.

230. Antonios JK, Yao Z, Li C, Rao AJ, Goodman SB. Macrophage polarization in response to wear particles in vitro. Cell Mol Immunol. 2013 Sep 9;10(6):cmi201339.

231. Rasmussen JW, Tam JW, Okan NA, Mena P, Furie MB, Thanassi DG, et al. Phenotypic, morphological, and functional heterogeneity of splenic immature myeloid cells in the host response to tularemia. Infect Immun. 2012 Jul;80(7):2371–81.

232. Kurts C. CD11c: not merely a murine DC marker, but also a useful vaccination target. Eur J Immunol. 2008 Aug;38(8):2072–5.

233. Singh-Jasuja H, Thiolat A, Ribon M, Boissier M-C, Bessis N, Rammensee H-G, et al. The mouse dendritic cell marker CD11c is down-regulated upon cell activation through Toll-like receptor triggering. Immunobiology. 2013 Jan 1;218(1):28–39.

234. Deng Z, Liu Y, Liu C, Xiang X, Wang J, Cheng Z, et al. Immature myeloid cells induced by a high-fat diet contribute to liver inflammation. Hepatol Baltim Md. 2009 Nov;50(5):1412–20.

235. Yang J, Zhang L, Yu C, Yang X-F, Wang H. Monocyte and macrophage differentiation: circulation inflammatory monocyte as biomarker for inflammatory diseases. Biomark Res. 2014 Jan 7;2:1.

236. van den Berg TK, Kraal G. A function for the macrophage F4/80 molecule in tolerance induction. Trends Immunol. 2005 Oct 1;26(10):506–9.

237. Yu Y-RA, O'Koren EG, Hotten DF, Kan MJ, Kopin D, Nelson ER, et al. A protocol for the comprehensive flow cytometric analysis of immune cells in normal and inflamed murine non-lymphoid tissues. PLoS ONE [Internet]. 2016 Mar 3 [cited 2017 Dec 11];11(3). Available from: https://www.ncbi.nlm.nih.gov/pmc/articles/PMC4777539/

238. Murray PJ, Wynn TA. Protective and pathogenic functions of macrophage subsets. Nat Rev Immunol. 2011 Oct 14;11(11):723–37.

239. Dendritic cell marker DCIR2 antibody, PE (monoclonal, 33D1) [Internet]. [cited 2017 Nov 20]. Available from: https://www.thermofisher.com/antibody/product/Dendritic-Cell-Marker-DCIR2-Antibody-clone-33D1-Monoclonal/12-5884-82

240. Walker JM. Gradient SDS polyacrylamide gel electrophoresis. Methods Mol Biol Clifton NJ. 1984;1:57–61.

241. Protein blotting guide [Internet]. Bio-Rad Laboratories, Inc.; Available from: www.bio-rad.com/webroot/web/pdf/lsr/literature/Bulletin_2895.pdf

242. Schonbrunn A. Editorial: Antibody can get it right: Confronting problems of antibody specificity and irreproducibility. Mol Endocrinol. 2014 Sep;28(9):1403–7.

243. Baker M. Reproducibility crisis: Blame it on the antibodies. Nat News. 2015 May 21;521(7552):274.

244. The fluorescent way: Why start fluorescent western blotting now? [Internet]. Bioradiations. 2017 [cited 2017 Nov 20]. Available from: http://www.bioradiations.com/the-fluorescent-way-why-start-fluorescent-western-blotting-now/

245. Yan Y. 7 - Growth of passive tribofilms in medical implants. In: Bio-Tribocorrosion in Biomaterials and Medical Implants [Internet]. Woodhead Publishing; 2013 [cited 2017 Dec 11]. p. 147–68. (Woodhead Publishing Series in Biomaterials). Available from: https://www.sciencedirect.com/science/article/pii/B9780857095404500077

246. Taira M, Sasaki K, Saitoh S, Nezu T, Sasaki M, Kimura S, et al. Accumulation of element Ti in macrophage-like RAW264 cells cultured in medium with 1 ppm Ti and effects on cell viability, SOD production and TNF-α secretion. Dent Mater J. 2006;25(4):726–32.

247. Alberts B, Johnson A, Lewis J, Raff M, Roberts K, Walter P. Studying gene expression and function. 2002 [cited 2017 Nov 20]; Available from: https://www.ncbi.nlm.nih.gov/books/NBK26818/

248. Curtis CD, Nardulli AM. Using RNA interference to study protein function. Methods Mol Biol Clifton NJ. 2009;505:187–204.

249. Shan G. RNA interference as a gene knockdown technique. Int J Biochem Cell Biol. 2010 Aug;42(8):1243–51.

250. Sledz CA, Williams BRG. RNA interference in biology and disease. Blood. 2005 Aug 1;106(3):787–94.

251. Aagaard L, Rossi JJ. RNAi therapeutics: Principles, prospects and challenges. Adv Drug Deliv Rev. 2007 Mar 30;59(2–3):75–86.

252. Rothman SS. Lessons from the living cell: The limits of reductionism. McGraw-Hill; 2002. 328 p.

253. Rao AJ, Zwingenberger S, Valladares R, Li C, Lane Smith R, Goodman SB, et al. Direct subcutaneous injection of polyethylene particles over the murine calvaria results in dramatic osteolysis. Int Orthop. 2013 Jul;37(7):1393–8.

254. Akbar M, Fraser AR, Graham GJ, Brewer JM, Grant MH. Acute inflammatory response to cobalt chromium orthopaedic wear debris in a rodent air-pouch model. J R Soc Interface. 2012 Sep 7;9(74):2109–19.

255. Ren W, Yang S-Y, Wooley PH. A novel murine model of orthopaedic wear-debris associated osteolysis. Scand J Rheumatol. 2004 Oct 1;33(5):349–57.

256. Hooper KA, Nickolas TL, Yurkow EJ, Kohn J, Laskin DL. Characterization of the inflammatory response to biomaterials using a rodent air pouch model. J Biomed Mater Res. 2000 Jun 5;50(3):365–74.

257. Gelb H, Schumacher HR, Cuckler J, Ducheyne P, Baker DG. In vivo inflammatory response to polymethylmethacrylate particulate debris: effect of size, morphology, and surface area. J Orthop Res Off Publ Orthop Res Soc. 1994 Jan;12(1):83–92.